Journal Pre-proofs

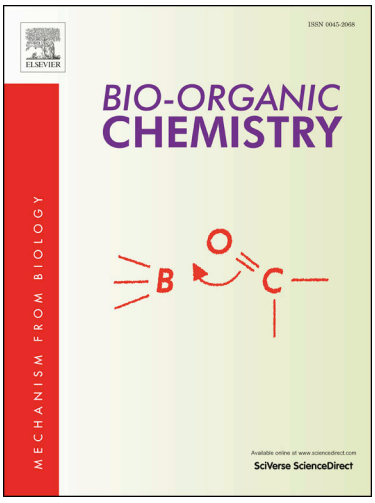

Discovery of Novel Dual c-Met/HDAC Inhibitors as a Promising Strategy for Cancer Therapy

Hao Hu, Fei Chen, Yuhong Dong, Yajing Liu, Ping Gong

PII: S0045-2068(20)30120-6
DOI: https://doi.org/10.1016/j.bioorg.2020.103970
Reference: YBIOO 103970

To appear in: *Bioorganic Chemistry*

Received Date: 16 January 2020
Revised Date: 21 May 2020
Accepted Date: 22 May 2020

Please cite this article as: H. Hu, F. Chen, Y. Dong, Y. Liu, P. Gong, Discovery of Novel Dual c-Met/HDAC Inhibitors as a Promising Strategy for Cancer Therapy, *Bioorganic Chemistry* (2020), doi: https://doi.org/10.1016/j.bioorg.2020.103970

Discovery of Novel Dual c-Met/HDAC Inhibitors as a Promising Strategy for Cancer Therapy

Hao Hu, Fei Chen, Yuhong Dong, Yajing Liu *, Ping Gong*[1]

Key Laboratory of Structure-Based Drug Design and Discovery (Shenyang Pharmaceutical University), Ministry of Education, 103 Wenhua Road, Shenhe District, Shenyang 110016, PR China

Abstract

Owing to the low efficacy and acquired resistance in clinical trials of c-Met inhibitors, based on the synergistic effects between c-Met and HDAC, novel c-Met and HDAC dual inhibitors were designed and synthesized. We introduced 2-pyrrolidinone to form the 5-atoms linker for c-Met inhibitor and hydroxamic acid as a zinc binding motif for HDAC inhibitor. The highly active dual inhibitor **15f** showed excellent and balanced activity against both c-Met (IC_{50} = 12.50 nM) and HDAC1 (IC_{50} = 26.97 nM). In those tested tumor cell lines, **15f** exhibits efficient antiproliferative activity with greater potency than Vorinostat (SAHA) and Cabozantinib (XL184). However, by comparing with an equimolar mixture of SAHA and Foretinib, we did not observe the compounds showed clearly synergistic antiproliferative effect. Nevertheless, compound **15f** was found to induce apoptosis and cause cell cycle arrest in G2/M phase. This proof-of-concept study provides an efficient strategy for discovery of multitarget antitumor drugs.

Keywords: c-Met; HDAC; 2-pyrrolidinone; antitumor drug

1. Introduction

Kinases are responsible for transferring phosphate groups from ATP to specific target molecules and have been the most intensively pursued classes of drug targets, especially in the treatment of cancers [1]. Since the discovery of protein kinase activity in 1954, the design and synthesis of different kinds of targeted cancer therapy drugs have advanced dramatically [2]. However, due to the multifaceted and dynamic nature of tumors, the foremost problem is that the effectiveness of kinase inhibitors is often impaired by acquired drug resistance [3-4]. It is reported that during the last three decades, the overall survival rates for cancer patients have not significantly improved owing to the emerging cancer resistance [5]. Cocktail therapy is one of the solutions to this problem, which was employed by clinicians to treat unresponsive patients [6]. Unfortunately, the approach of drug cocktails also resulted in

[1]Correspondence: Prof. Ping Gong and Yajing Liu, Key Laboratory of Structure-based Drug Design and Discovery, Ministry of Education, Shenyang Pharmaceutical University, Shenyang 110016, P. R. China.
E-mail: gongpinggp@126.com; lyjpharm@126.com.

complicated doses/schedule, unpredictable pharmacokinetic profile, drug-drug interactions, and reduced patient compliance [7-8]. From this point, a multitarget drug (single molecule) is an alternative approach to achieve multitarget therapy as compared to Cocktail therapy. Therefore, molecular hybridization paradigm is prevailing at present and becoming an interesting and smart way to defeat the multifaceted cancer disease.

c-Met [the receptor for hepatocyte growth factor/scatter factor, (HGF/SF)][9], which is composed of an extracellular α chain connected with a membrane-spanning β chain through a disulfide bond [10] is amplify or overexpress in various cancers that caused poor clinical outcomes[11-14] . In our previous study, based on a survey of launched and clinical c-Met inhibitors, we had designed series of quinoline derivatives and concluded the ‘‘5 atoms regulation’’ between moiety A and B **(Fig. 2)** [15-16]. However, similar to other RTK inhibitors, new research indicated that c-Met inhibition alone is usually not sufficient to block tumor progression due to complex factors, such as network robustness, bypass crosstalk, compensatory activities and acquired resistance in clinical trials [17].

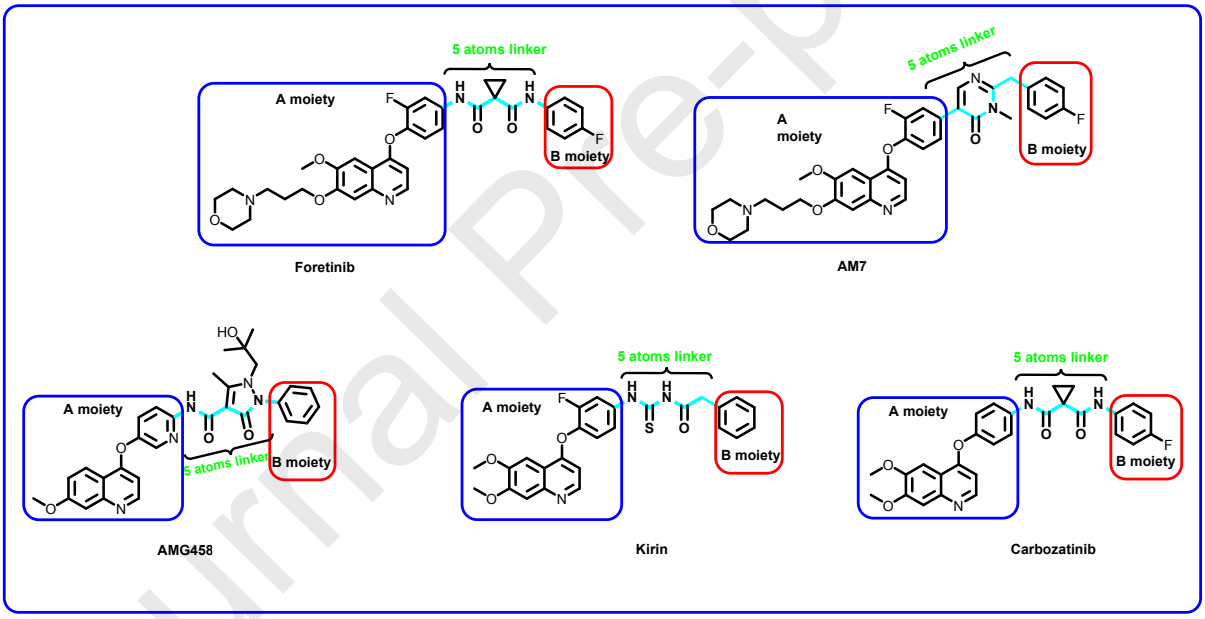

Fig. 2. The representative c-Met kinase inhibitors and the corresponding general structure.

It is easy to get discouraged when things are going bad. But we should not lose heart, because god is at work in our lives, even in the midst of pain and suffering. Fortunately, researchers have found the will of god which identified the histone deacetylases (HDACs) and told us the connection between HDAC signal and c-Met signal. HDACs play a crucial role in the regulation of multiple processes of life, from gene expressions transcription, cell proliferation, differentiation to protein activities [18]. More importantly, HDACs are also found to be overexpressed in some human cancers, so they are regarded as promising drug targets for several types of cancers therapy [19-20]. HDAC inhibition process affects c-Met and its downstream signaling pathways both directly and indirectly. In

literature researches, we also found HDAC inhibitors inhibit HGF production (the ligand of c-Met) [21]. As far as HDAC inhibitors are not only single epigenetic target anticancer drugs but also successful patterns as cytotoxic agents due to their familiar structures. Except for Romidepsin, almost all the HDAC inhibitors are sharing essential pharmacophoric structural features essential for the activity [22-23]. Therefore, it is so easy to link them to other anticancer scaffolds that many dual action HDAC inhibitors have been developed. Inspiringly, most of these hybrids have higher potency than the constituting parents in fighting of the cancer cells [24]. In this context, developments of dual HDAC inhibitors are proceeding intensively. There are a number of hybrid (chimeric) drugs that are currently in preclinical and clinical trials **(Fig. 1)**. CUDC-101 is a first-in-class hybrid inhibitor developed by Cai *et al* in 2010 which displayed potent *in vitro* inhibitory activity against HDAC1, EGFR and HER2 with an IC_{50} of 4.4, 2.4, and 15.7 nM, respectively [25]. CUDC-907 is a phosphatidylinositol 3-kinase (PI3K) and histone deacetylase (HDAC) inhibitor in phase II clinical trials at Curis for the treatment of relapsed or refractory diffuse large B-cell lymphoma (DLBCL) harboring MYC mutations [26-28]. Using successful RTK/HDAC hybrid inhibitor design, Lu *et al* reported the first potent c-Met and HDAC hybrid inhibitor 2m which inhibited c-Met kinase and HDAC1 with IC_{50} values of 0.71 and 38 nM, respectively [29].

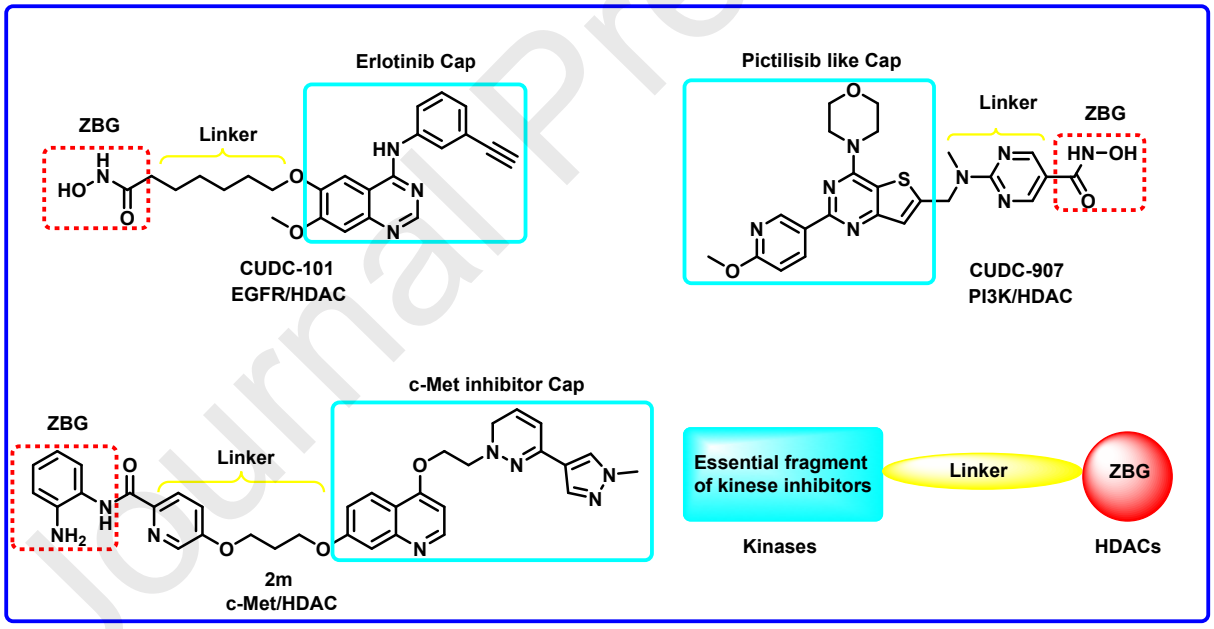

Fig. 1. Structures of representative dual RTK/HDAC inhibitors.

In this report, we present a fantastic idea for cancer drug development from a medicinal chemist's perspective, which hybrid the pharmacophores of HDACi with a c-Met inhibitor. On the basis of our knowledge and experience in the development of c-Met inhibitors, we found 2-pyrrolidinone fragment was widely used as a building block in the design of anticancer agents [30-31]. Furthermore, 2-pyrrolidinone fragment quite fit the "5 atoms regulation''. Moreover, in our previous studies, the six-carbon alkyl linker was found to be optimal for the dual inhibitors. In this

work, taking Foretinib as the lead compound, 2-pyrrolidinone was introduced to form the 5-atoms linker in order to promote c-Met activity. In addition, the hydroxamic acid side chain were introduced into solvent region of Foretinib being taken as the zinc-binding group (ZBG) of HDAC inhibitors [32] **(Fig. 3)**.

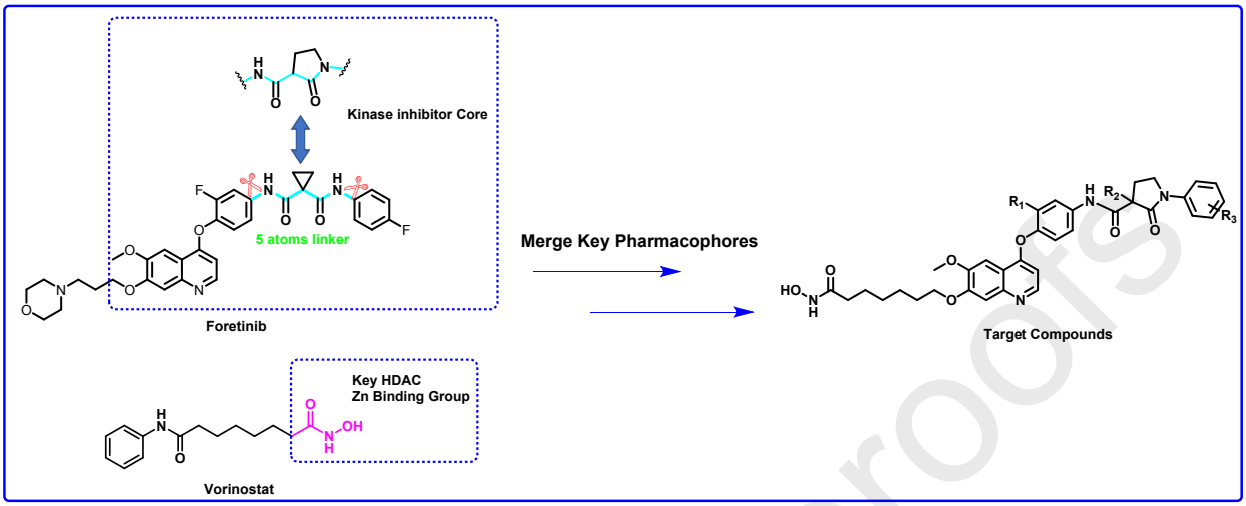

Fig. 3. Design strategy for the c-Met/HDAC dual inhibitors.

2. Results and discussion

2.1. Chemistry

*2.1.1. Synthesis of target compounds **15a-15t.***

The synthesis of c-Met/HDAC dual inhibitors are depicted in **Scheme 1**. The key intermediates **8a-8b** were treated with intermediates **12a-12s** to give condensed amide products **14a-14t**, respectively, which were treated with freshly prepared hydroxylamine methanol solution to give target compounds **15a-15t** [33].

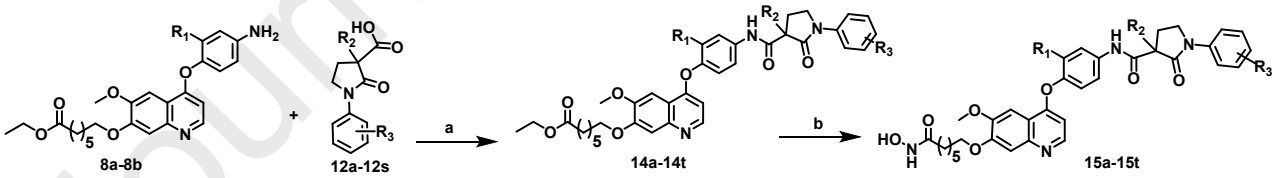

14a,15a: R_1=H,R_2=H,R_3=2,4-$(OCH_3)_2$	14b,15b: R_1=H,R_2=H,R_3=2-F	14c,15c: R_1=H,R_2=H,R_3=H	14d,15d: R_1=H,R_2=H,R_3=3,4-$(F)_2$
14e,15e: R_1=H,R_2=H, R_3=4-OCF_3	14f,15f: R_1=H,R_2=H,R_3= 4-F	14g,15g: R_1=H,R_2=H,R_3=2-OCH_3	14h,15h: R_1=H,R_2=H,R_3=4-$CH(CH_3)_2$
14i,15i: R_1=H,R_2=H,R_3=3-Cl,4-F	14j,15j: R_1=H,R_2=H,R_3=4-CH_2CH_3	14k,15k: R_1=H,R_2=H,R_3=2-OCF_3	14l,15l: R_1=H,R_2=H,R_3=4-Cl
14m,15m: R_1=H,R_2=H,R_3=4-Br	14n,15n: R_1=H,R_2=H,R_3= 3-F	14o,15o: R_1=H,R_2=H,R_3=2-Br	14p,15p: R_1=H,R_2=H,R_3=2-CH_3
14q,15q: R_1=F,R_2=H,R_3=H	14r,15r: R_1=H,R_2=CH_3,R_3=2-F	14s,15s: R_1=H,R_2=CH_3,R_3=H	14t,15t: R_1=H,R_2=CH_3,R_3=4-Cl

Scheme 1. Preparation of derivatives of **15a-15t**. Reagents and conditions:(a): HATU, Et_3N, DCM, 40 ℃, 3-5 h; (b): $NH_2OH{\cdot}HCl$, NaOH, anhydrous, CH_3OH, rt, 2-6 h;

The key intermediates **8a-8b** were synthesized as outlined in **Scheme 2.** Starting from commercially available acetovanillone **1** and ethyl 7-bromoheptanoate, intermediate **2** was prepared *via* a displacement reaction. The intermediate **2** treated with fuming nitric acid to obtain intermediate **3**. Intermediate **3** treated with DMF-DMA, Fe

powder, phosphorus oxychloride through acylation, cyclization and chlorination reaction to afforded intermediate **6. 7a-7b** were obtained through nucleophilic substitution with p-nitrophenol or 2-fluoro-4-nitrophenol in chlorobenzene, which were reduced by H_2/Pd to yield the desired intermediates **8a-8b**.

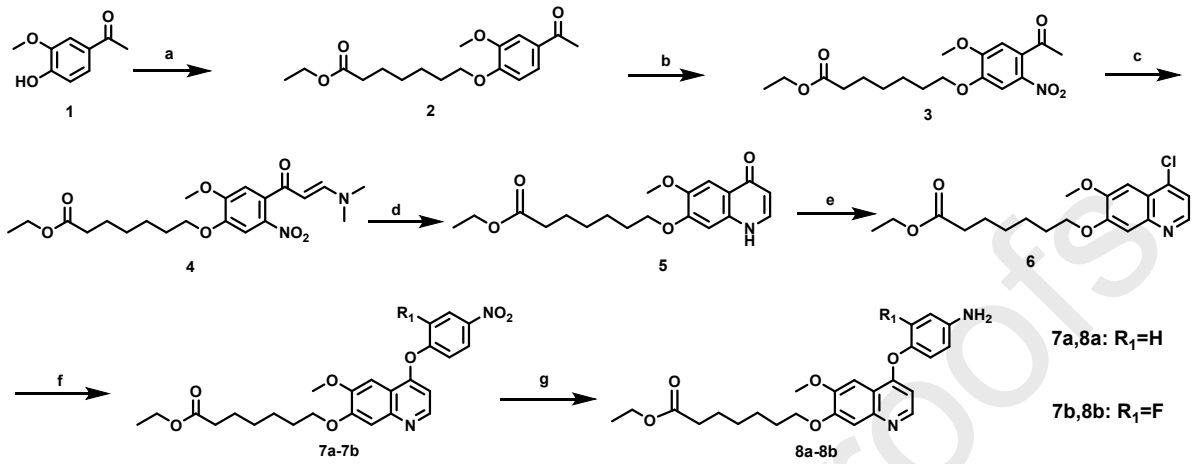

Scheme 2. Preparation of intermediates **8a-8b.** Reagents and conditions: (a) ethyl 7-bromoheptanoate, K_2CO_3, DMF, 80℃, 3-4 h;(b) fuming HNO_3, anhydrous DCM, -5 ℃, 6-8 h; (c) DMF-DMA, toluene, 110 °C, 7-8 h; (d) Fe powder, AcOH, r.t, 30 min, 80 °C, 1-2 h; (e) $POCl_3$, 85 ℃, 6-7 h; (f) 2-fluoro-4-nitrophenol/ *p*-nitrophenol, PhCl, 140 ℃, 20-24 h; (g) H_2, Pd/C(10%), CH_3OH,40 ℃, 3-5 h.

The intermediates **12a-12s** were synthesized as outlined in **Scheme 3** [34]. Briefly, cyclopropane-1,1-dicarboxylic acid reacted with acetone and acetic anhydride to afford intermediate **10**, which was reacted with different substituted anilines to obtain intermediates **12a-12p**, respectively. After treating **12b, 12c, 12l** with methyl iodide, intermediates **12q, 12s, 12t** were obtained.

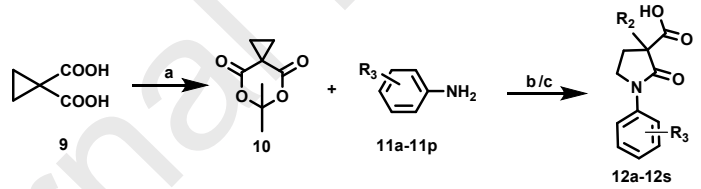

11a,12a: R_2=H, R_3=2,4-$(OCH_3)_2$	11b,12b, R_2=H, R_3=2-F	11c,12c: R_2=H, R_3=H	11d,12d: R_2=H, R_3=3,4-$(F)_2$
11e,12e: R_2=H, R_3=4-OCF_3	11f,12f: R_2=H, R_3= 4-F	11g,12g: R_2=H, R_3=2-OCH_3	11h,12h: R_2=H, R_3=4-$CH(CH_3)_2$
11i,12i: R_2=H, R_3=3-Cl,4-F	11j,12j: R_2=H, R_3=4-CH_2CH_3	11k,12k: R_2=H, R_3=2-OCF_3	11l,12l: R_2=H, R_3=4-Cl
11m,12m: R_2=H, R_3=4-Br	11n,12n: R_2=H, R_3= 3-F	11o,12o: R_2=H, R_3=2-Br	11p,12p: R_2=H, R_3=2-CH_3
11q,12q: R_2=CH_3, R_3=2-F	11s,12s:R_2=CH_3, R_3=H	11s,12s:R_2=CH_3, R_3=4-Cl	

Scheme 3. Preparation of intermediates **12a-12s.** Reagents and conditions: (a) i: conc H_2SO_4, Ac_2O, acetone, rt,10 h; (b) DMF, rt, 12 h; (c) THF, NaH, CH_3I, -5 ℃, 5 h;

2.2. Biological evaluation

2.2.1. HDAC1 and c-Met enzymatic activity assay

Initially, inhibitory activities for all compounds were preliminarily tested against c-Met and HDAC1 at 100 nM using compounds SAHA, XL-184 and Foretinib as reference drugs. The biological data listed in **Table 1** showed that most of the compounds exhibited excellent inhibitory activity against HDAC1, however, only seven compounds

inhibited c-Met over 50% rate at 100 nM.

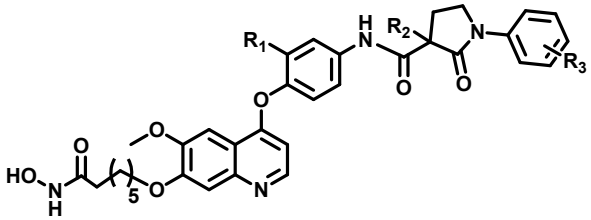

Table 1. HDAC1 and c-Met inhibitory activities of target compounds **15a-15t.**

Compd.	R_1	R_2	R_3	HDAC1 inhibition@100nM[a]	c-Met inhibition@100nM[a]
15a	H	H	2,4-$(OCH_3)_2$	79.8%	16.0%
15b	H	H	2-F	53.4%	57.0%
15c	H	H	H	35.9%	41.2%
15d	H	H	3,4-$(F)_2$	46.1%	40.1%
15e	H	H	4-OCF_3	18.9%	18.2%
15f	**H**	**H**	**4-F**	**77.8**%	**93.0**%
15g	H	H	2-OCH_3	78.4%	56.0%
15h	H	H	4-$CH(CH_3)_2$	21.6%	19.2%
15i	H	H	3-Cl,4-F	33.6%	26.4%
15j	H	H	4-CH_2CH_3	34.9%	51.7%
15k	H	H	2-OCF_3	61.1%	21.3%
15l	H	H	4-Cl	58.9%	41.0%
15m	H	H	4-Br	43.9%	14.4%
15n	H	H	3-F	77.9%	60.7%
15o	H	H	2-Br	71.5%	34.5%
15p	H	H	2-CH_3	67.6%	74.0%
15q	F	H	H	64.0%	82.1%
15r	H	CH_3	2-F	51.2%	12.5%
15s	H	CH_3	H	53.7%	39.0%

15t	H	CH_3	4-Cl	25.4%	15.0%
SAHA[b]				88.0%	NT
XL-184[b]				NT	91.6%
Foretinib[b]				NT	95.5%

[a] All compounds were assayed at least twice, and the inhibitory values were averaged.

[b] Used as a positive control.

NT= not tested.

As presented in **Table 1**, the effects of regiochemical substitution and electronics on the phenyl ring were explored. The introduction of electron-donating groups, such as methyl and methoxy, at the 2-position on the phenyl ring improve both HDAC1 and c-Met inhibition activity (**15g**, **15p** vs **15c**). Furthermore, by comparing compounds **15c** (HDAC1: inhibition rate 35.9 %; c-Met: inhibition rate 41.2%), **15h** (HDAC1: inhibition rate 21.6 %; c-Met: inhibition rate 19.2%) and **15f** (HDAC1: inhibition rate 77.8 %; c-Met: inhibition rate 93.0%), we could found that electron withdrawing group at the 4-position might contribute to the activity, while the electron donor might decrease inhibitory activity. Moreover, 4-position substituted compounds demonstrated the superior HDAC inhibitory activity than 3-position and 2-position substituted compounds (**15f** *vs* **15n** *vs* **15b**). In addition, introduction of double-electron-withdrawing groups (double-EWGs) or double-electron-donating groups (double-EDGs) on the phenyl ring both led to an obvious lost in c-Met activity comparing to the single substituent, such as compounds (**15a** *vs* **15g**, **15d** *vs* **15f**). Additionally, introducing steric hindrance at the 4-position of the phenyl ring decreased inhibitory activities (**15m** *vs* **15c**, **15h** *vs* **15c**).

Based on the previous report that halogen-containing substituents on the phenyl ring in the CUDC-101 displayed excellent inhibitory activities [25], we introduced F atom into R_1 to test their effects on inhibitory activities against HDAC1. From the result of **15c** and **15q**, we concluded that the introduction of fluorine atom was good for c-Met and HDAC1 inhibition.

Methylation is used to optimize many properties of a drug candidate. For example, methylating next to a metabolic hot spot might sterically block metabolism, lengthen the half-life. Methylation has a favorable effect on solubility or selectivity against off-targets. Indeed, methylation can have a favorable effect on binding affinity [35-36]. On the basis of the foregoing, our further investigations were performed to study the introduction of a methyl group to the 3 position of 2-pyrrolidinone core on the kinase activity. To our surprised, the compounds which containing a methyl group had a dramatic loss in activity (**15r** *vs* **15b**; **15s** *vs* **15c**; **15q** *vs* **15l**), The reason might be lay in that the preferred conformation was destructed by the introducing of methyl group.

Table 2. Enzymatic assays for HDAC1/c-Met inhibition.

Compd.	HDAC1 IC_{50} (nM) ± SD[a]	c-Met IC_{50} (nM) ± SD[a]
15f	26.97 ± 0.24	12.50 ± 0.42
15p	58.26 ± 1.15	42.24 ± 1.06
15q	76.24 ± 1.05	17.84 ± 0.25
SAHA[b]	14.15 ± 0.25	NT
XL-184[b]	NT	37.28 ± 1.10
Foretinib[b]	NT	2.11 ± 0.50

[a] SD: standard deviation.

[b] Positive control.

NT= not tested.

Compounds **15f**, **15p** and **15q** were select to screened half maximal inhibitory concentration (IC_{50}) against c-Met and HDAC1 kinases. As shown in **Table 2**, the tested compounds exhibited excellent c-Met and HDAC1 enzymatic potency with IC_{50} values in the nanomolar range. In particular, compound **15f** showed IC_{50} value against HDAC1 was 26.97 nM, which was less effective than SAHA (IC_{50} = 14.15 nM). However, the potency of **15f** against c-Met (IC_{50} = 12.50 nM) had been slightly improved than that of XL184 (IC_{50} = 37.28 nM), which validating our compound design strategy that incorporation of zinc binding group to the solvent-exposed phenyl group of Foretinib could obtain HDAC1 and c-Met dual inhibitory activities.

2.2.2. In vitro cytotoxic activities

To further explore the antitumor effect of these c-Met/HDAC inhibitors, all dual inhibitors were tested against a panel of three solid tumor cell lines selected as representative of hard-to-treat solid tumors while being known to be sensitive to c-Met and HDAC inhibitors: HCT-116 (human colon cancer), A549 (human lung adenocarcinoma) and MCF-7 (human breast cancer) by MTT assay.

Table 3. The antiproliferative activities of **15a-15t** against HCT-116, MCF-7and A549 cell lines in *vitro*.

Compd.	R_1	R_2	R_3	IC_{50} [a] (μmol/L) ± SD		
				HCT-116	MCF-7	A549
15a	H	H	2,4-$(OCH_3)_2$	11.90 ± 0.26	2.06 ± 0.21	>20

15b	H	H	2-F	2.68 ± 0.05	0.57 ± 0.03	1.12 ± 0.10
15c	H	H	H	3.45 ± 0.22	0.74 ± 0.10	3.99 ± 0.15
15d	H	H	3,4-$(F)_2$	2.12 ± 0.02	1.93 ± 0.20	4.44 ± 0.12
15e	H	H	4-OCF_3	3.37 ± 0.19	0.77 ± 0.04	8.28 ± 1.21
15f	**H**	**H**	**4-F**	**0.54 ± 0.05**	**0.28 ± 0.02**	**1.08 ± 0.44**
15g	H	H	2-OCH_3	3.73 ± 0.12	1.86 ± 0.01	5.60 ± 0.33
15h	H	H	4-$CH(CH_3)_2$	1.68 ± 0.43	0.80 ± 0.01	10.05 ± 0.55
15i	H	H	3-Cl,4-F	3.55 ± 0.06	2.30 ± 1.10	18.92 ± 1.50
15j	H	H	4-CH_2CH_3	5.07 ± 0.34	1.44 ± 0.05	6.79 ± 0.10
15k	H	H	2-OCF_3	7.18 ± 0.25	0.78 ± 0.44	2.08 ± 0.34
15l	H	H	4-Cl	0.14 ± 0.02	1.72 ± 0.47	3.86 ± 0.05
15m	H	H	4-Br	3.99 ± 0.04	1.39 ± 0.06	4.38 ± 0.20
15n	H	H	3-F	0.47 ± 0.03	0.77 ± 0.05	1.92 ± 0.31
15o	H	H	2-Br	4.08 ± 0.25	1.77 ± 0.21	6.76 ± 0.24
15p	H	H	2-CH_3	0.42 ± 0.06	2.02 ± 0.40	1.98 ± 1.00
15q	F	H	H	2.10 ± 0.08	1.14 ± 0.09	1.76± 0.29
15r	H	CH_3	2-F	9.01 ± 0.52	3.52 ± 0.24	>20
15s	H	CH_3	H	7.29 ± 0.38	5.51 ± 0.05	9.97 ± 1.02
15t	H	CH_3	4-Cl	3.52 ± 0.12	1.57 ± 0.05	8.43 ± 0.02
SAHA[b]				0.68 ± 0.13	0.99 ± 0.20	2.29 ± 0.05
XL-184[b]				4.50 ± 0.08	5.58 ± 0.15	7.34 ± 0.20
Foretinib[b]				0.63 ± 0.09	0.52 ± 0.08	0.94 ± 0.04
SAHA+Foretinib (1:1)				0.64 ± 0.12	0.62 ± 0.11	0.99 ± 0.06

[a] Inhibition values represent the average of at least three independent experiments.

[b] Used as a positive control.

Data in **Table 3** illustrated that the target compounds exhibited moderate to potent antiproliferation activities against one or more tested cancer cell lines with potencies in the single digit micromole range, which was mostly in accordance with the trend in enzymatic activity. However, by comparing with an equimolar mixture of SAHA and Foretinib, we did not observe the compounds showed clearly synergistic effect. Interestingly, among the tested solid tumor cell lines, the human breast cancer cell line MCF-7 seemed to be the most sensitive one to our compounds, indicating that the target compounds might be used in curing human breast cancer. Among them, compound **15f** exhibited the best activity against all of the tested cell lines with IC_{50} value of 0.54, 0.28 and 1.08 μM against HCT-116, MCF-7 and A549 cell lines, respectively, indicating that **15f** deserve further study with regard to its application in the treatment of cancer.

2.2.3. Cell apoptosis study

To further explore whether our compounds are accompanied by enhanced cancer cell apoptosis, we then performed a FITC-Annexin V/propidium iodide (PI) staining and flow cytometry assay of **15f** in HCT-116 cells. As shown in **Fig. 4**, 3.01% apoptotic cells were observed in control group treated with DMSO, whereas tumor cells treated with **15f** at defined concentrations of 0.2, 1.0 and 5.0 μM for 48 h resulted in 6.97%, 7.08% and 13.21% cells apoptosis, respectively. The results showed that compound **15f** increased the cellular apoptosis in a concentration dependent manner, which might result from concerted inhibition of c-Met and HDAC1 activity.

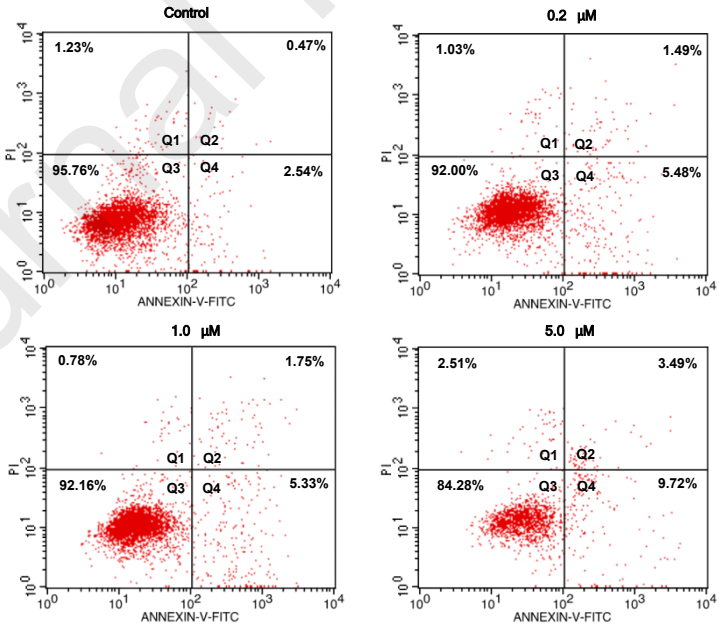

Fig. 4. Compound **15f** induced apoptosis in HCT-116 cells. Cells were treated with various concentrations of **15f** for 48 h and then analyzed the Annexin V-FITC/PI staining test by flow cytometry analysis. Values represent the mean ± S.D, n = 3. The percentage of cells in each part is indicated.

2.2.4. Cell cycle analysis

To evaluate whether **15f** could induce tumor cell cycle arrest, we then performed a flow cytometry assay to assess the effect of **15f** on the distribution of cell cycle. The cell cycle profiles of HCT-116 after treating with **15f** in different concentrations for 48 h, and the results were illustrated in **Fig. 5-6**. It is clearly disclosed that **15f** showed an obvious increase in the proportion of cells in G2/M phase in a dose-dependent manner. The percentage of cells in G2/M phase was gradually increased from 10.61% in the untreated cells to 86.68%, 88.36% and 87.75% in cells treated with **15f** at 0.2, 1.0 and 5.0 μM, respectively.

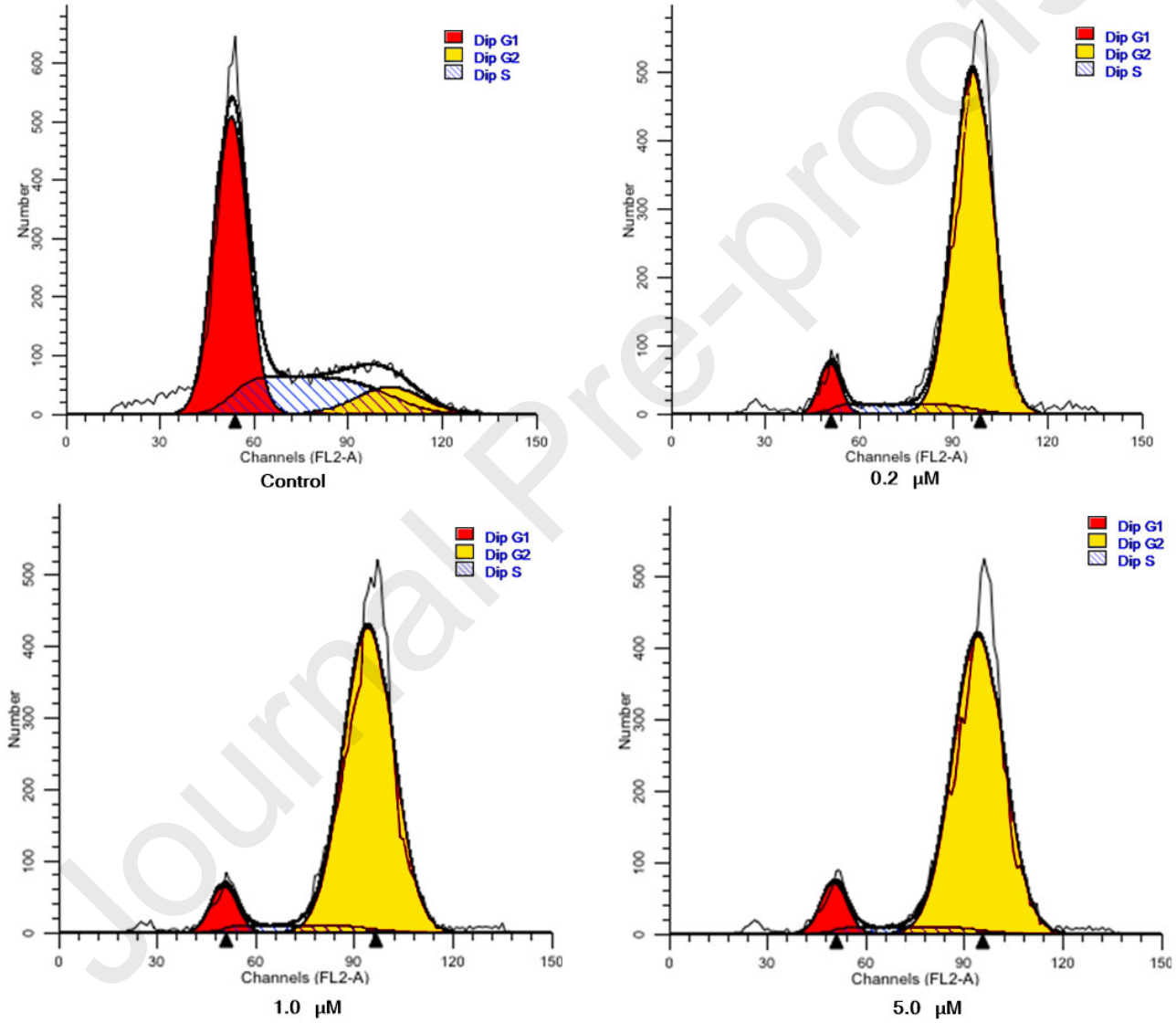

Fig. 5. Effect of compound **15f** on the cell cycle distribution of HCT-116 cells. The experiments were performed three times and a representative experiment is shown.

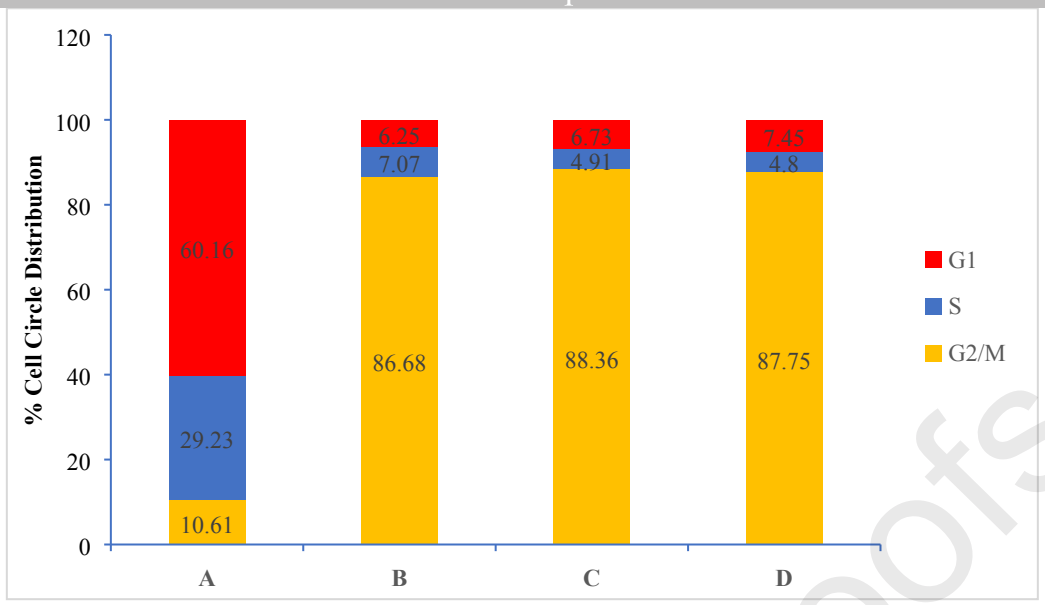

Fig. 6. Quantitative analysis of cell cycle distributions; (**A**) Non-treated cells as control group (**B**) treated with **15f** at 0.2 μM (**C**) treated with **15f** at 1.0 μM (**D**) treated with **15f** at 5.0 μM

2.2.5. Binding Mode of the c-Met/HDAC Dual Inhibitor.

Docking simulations were performed for the selected compound **15f** to investigate whether it can form favorite interactions with the two targets. The best-scored pose of compound **15f** with c-Met and HDAC1 are presented in **Fig.7**. For the binding mode of **15f** with HDAC1 (PDB ID:1C3S, **Fig.7 A, B**) [37], the hydroxamic acid coordinated to the catalytic Zn^{2+} of HDAC1 and formed a hydrogen bond with His131. The molecular docking with **15f** in c-Met (PDB ID:3LQ8) was also performed [32], the result was shown in **Fig.7 C, D.** The carbonyl of the amide hydrogen bond with the residue of Lys1110. In addition, the carbonyl of pyrrolidinone formed hydrogen bond with the residues of Asp1222. The N atom of quinoline ring of **15f** made hydrogen bond with Met1160 in the hinge region. Furthermore, the hydroxamic tail formed two hydrogen bonds with the residues of His1162 and Lys1161.

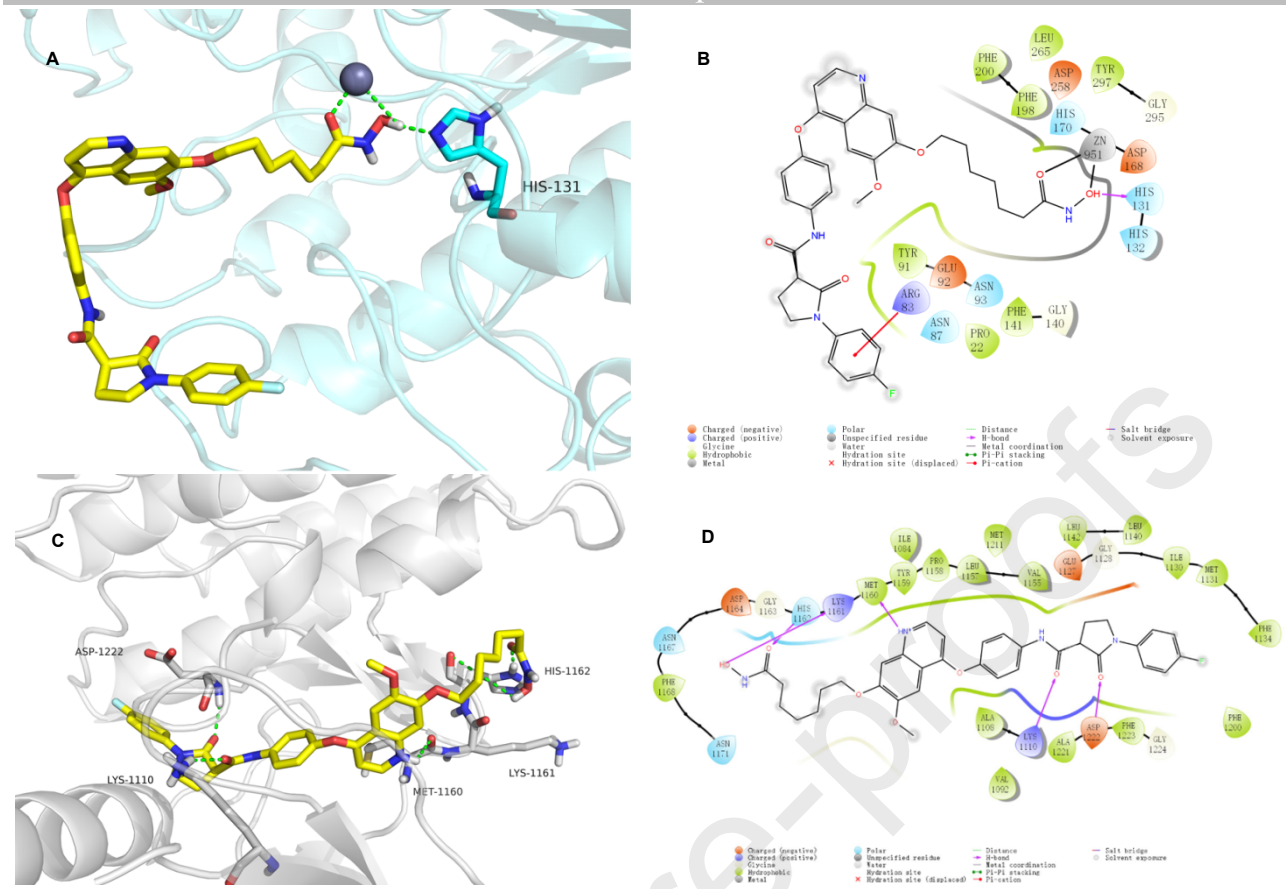

Fig. 7. (A) Proposed 3D binding mode of compound **15f** in the active site of HDAC1 (PDB: 1C3S). **(B)** Proposed 2D binding mode of compound **15f** in the active site of HDAC1 (PDB: 1C3S). (**C**) Proposed 3D binding mode of compound **15f** in the active site of c-Met (PDB: 3LQ8). (**D**) Proposed 2D binding mode of compound **15f** in the active site of c-Met (PDB: 3LQ8). The figure was generated using PyMol (http://www.pymol.org).

3. Conclusions

On the basis of the pharmacophore fusion strategy, through designing and structural optimization targeting on c-Met and HDAC1, we finally discovered a new compound **15f** which potently inhibited c-Met and HDAC1 with IC_{50} values of 12.50 and 26.97 nM, respectively. In *vitro* cellular assays, **15f** showed potent activities against HCT-116, MCF-7 and A549 cell lines with IC_{50} values of 0.54, 0.28 and 1.08 μM, respectively. Antitumor mechanism studies showed that **15f** could promote induction of apoptosis in a dose-dependent manner. Moreover, **15f** could block the G2/M phase even at 0.2 μM. The molecular docking analysis can be used as a valuable probe to clarify the two enzymes inhibitory activity. All the studies indicated **15f** as a novel "hit" compound targeting on c-Met and HDAC1 deserve for further investigation and development.

4. Experimental

4.1. Chemistry

Unless otherwise specified, all materials were obtained from commercial suppliers and were used without further purification. Reactions' time and purity of the products were monitored by TLC on FLUKA silica gel aluminum cards (0.2 mm thickness) with fluorescent indicator 254 nm. Column chromatography was run on silica gel (200–300 mesh) from Qingdao Ocean Chemicals (Qingdao, Shandong, China). All melting points were obtained on a Büchi Melting Point B-540 apparatus (Büchi Labortechnik, Flawil, Switzerland) and were uncorrected. Mass spectra (MS) were taken in ESI mode on Agilent 1100 LC–MS (Agilent, Palo Alto, CA, USA). ^{1}HNMR and ^{13}C NMR spectra were performed using Bruker spectrometers (BrukerBioscience, respectively, Billerica, MA, USA) with TMS as an internal standard.

*4.1.1. Preparation of ethyl 7-(4-acetyl-2-methoxyphenoxy)heptanoate (**2**)*

To a solution of 4-hydroxy-3-methoxy-acetophenone (20.0 g, 120.5 mmol) in DMF (200 mL) was added K_2CO_3 (17.4 g, 126.5 mmol) and ethyl 7-bromoheptanoate (30.0 g, 126.5 mmol). The reaction mixture was then stirred at 80 °C for 4 h. The mixture was then poured into cold water (500 mL) with vigorously agitating, the resulting precipitate was filtered-off, washed with water, and dried under vacuum to afford the title compound **2** (31.3 g, 80.1%) as a white solid. MS (ESI) m/z: 323.05 $[M+H]^+$.

*4.1.2. Preparation of ethyl 7-(4-acetyl-2-methoxy-5-nitrophenoxy)heptanoate (**3**)*

A stirred solution of **2** (30.0 g, 93.1 mmol) in CH_2Cl_2 (300 mL) was cooled to 10 °C, fuming HNO_3 (43.5 g, 465.5 mmol) was added at an appropriate rate keeping the temperature below -5 °C. The reaction mixture was allowed to stir at -5 °C for 6 h, then poured into cold water (200 mL), the organic layer was separated and washed with water (200 mL), then concentrated under reduced pressure to afford crude **3** as a light yellow solid (29.3 g, 85.7%). MS (ESI) m/z: 390.04 $[M+Na]^+$.

*4.1.3. Preparation of ethyl (E)-7-(4-(3-(dimethylamino)acryloyl)-2-methoxy-5-nitrophenoxy)heptanoate (**4**)*

28.0 g (76.3 mmol) of **3** was suspended in 280 mL of toluene at room temperature, then DMF-DMA (24.0 g, 228.9 mmol) was added to a solution. The reaction was heated to 110 °C for 4 h. After cooling to rt, the resultant solid was collected by filtration, washed with toluene (40 mL), then dried under vacuum to yield **4** as a yellow solid (24.4 g, 75.8%). MS (ESI) m/z: 445.05 $[M+Na]^+$.

*4.1.4. Preparation of ethyl 7-((6-methoxy-4-oxo-1,4-dihydroquinolin-7-yl)oxy)heptanoate (**5**)*

Fe powder (15.9 g, 284.2 mmol) was added to a solution of **4** (24.0 g, 56.8 mmol) in acetic acid (100 mL) at 60 °C in batches, then the mixture was stirred at 80 °C for 2 h. The hot solution was filtered through celite and washed with hot acetic acid. The combined filtrate was cooled to rt, the resultant solid was collected by filtration and washed with acetic acid (50 mL) to afford **5** as a yellow solid (12.4 g, 62.9 %). MS (ESI) m/z: 348.02 [M+H]

$^{+}$.

*4.1.5. Preparation of ethyl 7-((4-chloro-6-methoxyquinolin-7-yl)oxy)heptanoate (**6**)*

A mixture consisting of 12.0 g (34.6 mmol) **5** and 96.0 mL (8 v/m) phosphorus oxychloride was refluxed for 10 h whereby a clear solution was formed. Thereafter, the excess unreacted phosphorus oxychloride was evaporated in vacuo and the residual oil was poured into ice water. The precipitate formed under vigorous stirring conditions, thereby the solid was collected by vacuum filtration, dried under reduced pressure to afford product **6** as a pale solid (10.1 g, 80.2%). ^{1}H NMR (600 MHz, DMSO-d_6) δ 8.56 (d, J = 4.8 Hz, 1H), 7.48 (d, J = 4.8 Hz, 1H), 7.37 (s, 1H), 7.29 (s, 1H), 4.09 (t, J = 6.5 Hz, 2H), 4.03 (q, J = 7.1 Hz, 2H), 3.94 (s, 3H), 2.26 (t, J = 7.4 Hz, 2H), 1.76 (t, J = 7.4 Hz, 2H), 1.58 – 1.48 (m, 2H), 1.42 (t, J = 7.8 Hz, 2H), 1.32 (q, J = 8.4 Hz, 2H), 1.15 (t, J = 7.1 Hz, 3H).

*4.1.6. General procedure for the preparation of intermediates (**7a-7b**)*

4-nitrophenol (4.1 g, 29.6 mmol) or 2-fluoro-4-nitrophenol (4.6 g, 29.6 mmol) was added to a stirred solution of **6** (9.0 g, 24.7 mmol) in 60 mL chlorobenzene, then the reaction mixture was refluxed for 24 h whereby a clear solution was formed. Then evaporated in vacuo, the resulting precipitate was added to 100 mL DCM, the organic portion was washed with 10% w/w aqueous sodium bicarbonate solution (3 x 50 mL), the organic layer was evaporated in vacuo and dried under reduced pressure to afford product **7a-7b.**

*4.1.6.1. ethyl 7-((6-methoxy-4-(4-nitrophenoxy)quinolin-7-yl)oxy)heptanoate(**7a**)*

Yellow solid, yield 52.5%, MS (ESI) m/z (%): 469.00 $[M+H]^{+}$; ^{1}H NMR (600 MHz, DMSO-d_6) δ 8.42 (d, J = 5.3 Hz, 1H), 7.50 (s, 1H), 7.34 (s, 1H), 6.93 (d, J = 8.7 Hz, 2H), 6.67 (d, J = 8.8 Hz, 2H), 6.36 (d, J = 5.2 Hz, 1H), 5.18 (s, 2H), 4.12 (t, J = 6.5 Hz, 2H), 4.05 (q, J = 7.1 Hz, 2H), 3.93 (s, 3H), 2.30 (t, J = 7.4 Hz, 2H), 1.80 (p, J = 6.7 Hz, 2H), 1.57 (p, J = 7.4 Hz, 2H), 1.47 (p, J = 7.5 Hz, 2H), 1.37 (q, J = 8.1 Hz, 2H), 1.18 (t, J = 7.1 Hz, 3H).

*4.1.6.2. ethyl 7-((4-(2-fluoro-4-nitrophenoxy)-6-methoxyquinolin-7-yl)oxy)heptanoate (**7b**)*

Yellow solid, yield 56.8%, MS (ESI) m/z (%): 487.12 $[M+H]^{+}$.

*4.1.7. General procedure for the preparation of intermediates (**8a-8b**)*

10% Pd/C (0.5 g, 10%w/w) was added to a stirred solution of **7a** or **7b** (5.0 g) in 50 mL methanol under H_2, then the mixture was stirred at 40 °C for 4 h. After completion of reaction, it was allowed to cool to room temperature. The solution was filtered through celite and washed with methanol (10 mL), then solvent was evaporated in vacuo and dried under reduced pressure to afford product **8a-8b**.

*4.1.7.1. ethyl 7-((4-(4-aminophenoxy)-6-methoxyquinolin-7-yl)oxy)heptanoate (**8a**)*

Yellow solid, yield 91.7% ,MS (ESI) m/z (%): 439.19 $[M+H]^{+}$.

*4.1.7.2. ethyl 7-((4-(4-amino-2-fluorophenoxy)-6-methoxyquinolin-7-yl)oxy)heptanoate (**8b**)*

Yellow solid, yield 89.8% ,MS (ESI) m/z (%): 457.22 $[M+H]^+$.

*4.1.8. Preparation of 6,6-dimethyl-5,7-dioxaspiro[2.5]octane-4,8-dione (**10**)*

10.0 g (76.9 mmol) of cyclopropane-1,1-dicarboxylic acid (**9**) was added together with (9.5 ml, 92.3 mmol) of acetic anhydride and 0.25 ml of sulfuric acid and heated at 30 to 35 °C. Then (7.5 ml, 92.3 mmol) of acetone is added dropwise, the temperature of the reaction mixture is kept at 30 to 35 °C. After completion of the addition of acetone, the reaction mixture is stirred for about 8 hours at 30 to 35 °C. The reaction mixture poured into 100 mL ice-water, a white crystalline was obtained by filtration. The solid was twice washed with 30 ml portions of cold water, then dried under reduced pressure to afford product **10** as a white solid (10.6 g, 81.5 %). MS (ESI) m/z: 171.23 $[M+H]^+$.

*4.1.9. General procedure for preparation intermediates (**12a-12p**)*

To a solution of 6,6-dimethyl-5,7-dioxaspiro[2.5]octane-4,8-dione (1.0 g, 5.9 mmol) in 10 mL of DMF was added substituted aniline **11a-11p** (6.5 mmol). The reaction mixture was stirred at rt overnight. The reaction mixture was poured into cold water (10 mL). The precipitate that formed was collected by filtration, washed with water, and dried under vacuum to afford the desired product **12a-12p**.

*4.1.9.1. Preparation of 1-(2,4-dimethoxyphenyl)-2-oxopyrrolidine-3-carboxylic acid (**12a**)*

Gray solid; yield: 81.2%; MS (ESI) m/z: 266.17 $[M+H]^+$.

*4.1.9.2. Preparation of 1-(2-fluorophenyl)-2-oxopyrrolidine-3-carboxylic acid (**12b**)*

White solid; yield: 89.4%; MS (ESI) m/z: 224.17 $[M+H]^+$.

*4.1.9.3. Preparation of 2-oxo-1-phenylpyrrolidine-3-carboxylic acid (**12c**)*

White solid; yield: 84.3%; MS (ESI) m/z: 206.16 $[M+H]^+$; ^{1}H NMR (600 MHz, DMSO-d_6) δ 12.74 (s, 1H), 7.70 – 7.58 (m, 2H), 7.45 – 7.32 (m, 2H), 7.22 – 7.11 (m, 1H), 3.95 – 3.78 (m, 2H), 3.60 (dd, J = 9.1, 7.8 Hz, 1H), 2.42 – 2.22 (m, 2H).

*4.1.9.4. Preparation of 1-(3,4-difluorophenyl)-2-oxopyrrolidine-3-carboxylic acid (**12d**)*

Yellow solid; yield: 74.4%; MS (ESI) m/z: 242.17 $[M+H]^+$; ^{1}H NMR (600 MHz, DMSO-d_6) δ 12.89 (s, 1H), 7.85 (ddd, J = 12.1, 6.8, 2.1 Hz, 1H), 7.53 – 7.37 (m, 2H), 3.89 (m, 1H), 3.83 (m, 1H), 3.63 (m, 1H), 2.34 (dd, J = 36.1, 8.2 Hz, 2H).

*4.1.9.5. Preparation of 2-oxo-1-(4-(trifluoromethoxy)phenyl)pyrrolidine-3-carboxylic acid (**12e**)*

White solid; yield: 75.0%; MS (ESI) m/z: 290.16 $[M+H]^+$.

*4.1.9.6 Preparation of 1-(4-fluorophenyl)-2-oxopyrrolidine-3-carboxylic acid (**12f**)*

White solid; yield: 74.1%; MS (ESI) m/z: 224.17 $[M+H]^+$.

*4.1.9.7. Preparation of 1-(4-methoxyphenyl)-2-oxopyrrolidine-3-carboxylic acid (**12g**)*

Yellow solid; total yield: 82.5%; MS (ESI) m/z: 236.20 $[M+H]^+$.

*4.1.9.8. Preparation of 1-(4-isopropylphenyl)-2-oxopyrrolidine-3-carboxylic acid (**12h**)*

White solid; yield: 80.1%; MS (ESI) m/z: 248.23 $[M+H]^+$.

*4.1.9.9. Preparation of 1-(3-chloro-4-fluorophenyl)-2-oxopyrrolidine-3-carboxylic acid (**12i**)*

White solid; yield: 67.5%; MS (ESI) m/z: 258.17 $[M+H]^+$.

*4.1.9.10. Preparation of 1-(4-ethylphenyl)-2-oxopyrrolidine-3-carboxylic acid (**12j**)*

White solid; yield: 83.1%; MS (ESI) m/z: 234.18 $[M+H]^+$.

*4.1.9.11. Preparation of 2-oxo-1-(2-(trifluoromethoxy)phenyl)pyrrolidine-3-carboxylic acid (**12k**)*

White solid; yield: 72.3%; MS (ESI) m/z: 290.16 $[M+H]^+$.

*4.1.9.12. Preparation of 1-(4-chlorophenyl)-2-oxopyrrolidine-3-carboxylic acid (**12l**)*

White solid; yield: 81.6%; MS (ESI) m/z: 240.16 $[M+H]^+$.

*4.1.9.13. Preparation of 1-(4-bromophenyl)-2-oxopyrrolidine-3-carboxylic acid (**12m**)*

White solid; yield: 70.6%; MS (ESI) m/z: 284.05 $[M+H]^+$.

*4.1.9.14. Preparation of 1-(3-fluorophenyl)-2-oxopyrrolidine-3-carboxylic acid (**12n**)*

White solid; yield: 79.9%; MS (ESI) m/z: 224.24 $[M+H]^+$.

*4.1.9.15. Preparation of 1-(2-bromophenyl)-2-oxopyrrolidine-3-carboxylic acid (**12o**)*

White solid; yield: 69.1%; MS (ESI) m/z: 284.05 $[M+H]^+$.

*4.1.9.16. Preparation of 2-oxo-1-(o-tolyl)pyrrolidine-3-carboxylic acid (**12p**)*

White solid; yield: 88.1%; MS (ESI) m/z: 220.21 $[M+H]^+$.

*4.1.10. General procedure for preparation intermediates (**12q, 12r, 12s**)*

Appropriate intermediate **12b, 12c, 12l** (10.0 mmol) was suspended in 20 mL of dry tetrahydrofuran at -5°C, NaH(0.72 g, 30.0 mmol) was added in batches. After stirring for 0.5 h at -5 °C, CH_3I (2.1 g, 15.0 mmol) was added at an appropriate rate keeping the temperature below 0-5 °C. After completion of the addition, the reaction mixture was stirred for about 2 h at rt. The reaction mixture poured into 100 mL ice-water, acidized to pH 2-3 with 6 N HCl, the precipitate that formed was collected by filtration, washed with water, and dried under vacuum to afford the desired product.

*4.1.10.1. Preparation of 1-(2-fluorophenyl)-3-methyl-2-oxopyrrolidine-3-carboxylic acid (**12q**)*

White solid; yield: 56.2%, MS (ESI) m/z (%): 238.15 $[M+H]^+$;

*4.1.10.2. Preparation of 3-methyl-2-oxo-1-phenylpyrrolidine-3-carboxylic acid (**12r**)*

White solid; yield: 62.7%, MS (ESI) m/z (%): 220.14 $[M+H]^+$.

*4.1.10.3. Preparation of 1-(4-chlorophenyl)-3-methyl-2-oxopyrrolidine-3-carboxylic acid (**12s**)*

White solid; yield: 74.0%, MS (ESI) m/z (%): 254.14 $[M+H]^+$.

*4.1.11. General procedure for preparation of intermediates (**14a-14t**)*

A mixture of **8a-8b** (1.0 mmol) and different intermediates **12a-12s** (1.3 mmol), HATU (1.3 mmol), TEA (1.3 mmol) in DCM (15 mL) was stirred at reflux for 3-5 h. After being cooled to rt, the mixture was washed successively with 10% aqueous potassium carbonate solution (20 mL×3) and brine (20 mL×2), the organic phase was dried over anhydrous sodium sulfate. The solid was removed by filtration, and the filtrate was concentrated to yield the **14a-14t**, respectively, yeilds 60.7-92.2%. Without any purification, the intermediates were used for next procedure.

*4.1.12. General procedure for preparation of target compounds (**15a-15t**)*

A solution of sodium hydroxide (4.0 g, 100.0 mmol) in methanol (14 mL) was added to a stirred solution of hydroxylamine hydrochloride (4.7 g, 67.2 mmol) in methanol (24 mL) at 0 °C. The reaction mixture was stirred at 0 °C for 1 h. The precipitate was removed by filtration and the filtrate was collected to provide fresh hydroxylamine solution which was stored in a refrigerator before use. The appropriate intermediates **14a-14t** (1.0 mmol) was added to the above freshly prepared hydroxylamine solution (15 mL) at 0 °C, then NaOH (0.04 g,1.0 mmol) was added to the solution. The reaction mixture was stirred at room temperature for 2-6 h. The reaction mixture was neutralized with 6 N HCl. The formed precipitate was collected by filtration, washed with water, dried in vacuo and purified by silica gel chromatography to afford target compounds **15a-15t**.

*4.1.12.1. 1-(2,4-dimethoxyphenyl)-N-(4-((7-((7-(hydroxyamino)-7-oxoheptyl)oxy)-6-methoxyquinolin-4-yl)oxy)phenyl)-2-oxopyrrolidine-3-carboxamide (**15a**)*

Gray solid; Yield: 64.1%; M.p.: 115-116 °C; MS (ESI) m/z(%): 673.26 $[M+H]^+$; ^{1}H NMR (600 MHz, DMSO-d_6) δ 10.43 (s, 1H), 10.37 (s, 1H), 8.71 (s, 1H), 8.45 (d, J = 5.2 Hz, 1H), 7.80 (d, J = 8.4 Hz, 2H), 7.52 (s, 1H), 7.38 (s, 1H), 7.26 (d, J = 8.4 Hz, 2H), 7.12 (d, J = 8.6 Hz, 1H), 6.67 (d, J = 2.6 Hz, 1H), 6.56 (dd, J = 8.6, 2.6 Hz, 1H), 6.45 (d, J = 5.2 Hz, 1H), 4.13 (m, 4H), 3.94 (s, 3H), 3.79 (d, J = 5.1 Hz, 6H), 3.66 (m, 2H), 2.33 (m, 1H), 1.98 (t, J = 7.3 Hz, 2H), 1.81 (t, J = 7.4 Hz, 2H), 1.54 (t, J = 7.6 Hz, 2H), 1.49 – 1.42 (m, 2H), 1.35 (dt, J = 13.9, 6.5 Hz, 2H). ^{13}C NMR (101 MHz, DMSO-d_6) δ 171.37 , 169.60 , 168.15 , 160.42 , 160.24 , 156.06 , 152.37 , 149.93 , 149.78 , 149.23 , 146.88 , 136.99 , 129.54 , 121.95 , 121.29 , 120.32 , 115.50 , 108.91 , 105.36 , 103.45 , 99.90 , 99.62 , 68.70 , 56.22 , 55.89 , 49.75 , 49.06 , 48.57 , 32.71 , 28.87 , 28.80 , 25.75 , 25.55 , 22.50 .

*4.1.12.2. 1-(2-fluorophenyl)-N-(4-((7-((7-(hydroxyamino)-7-oxoheptyl)oxy)-6-methoxyquinolin-4-yl)oxy)phenyl)-2-oxopyrrolidine-3-carboxamide (**15b**)*

White solid; Yield: 46.4%; M.p.: 138-139 ºC; MS (ESI) m/z(%): 631.14 $[M+H]^+$; ^{1}H NMR (400 MHz, DMSO-d_6) δ 10.50 (s, 1H), 10.35 (s, 1H), 8.68 (s, 1H), 8.46 (d, J = 5.2 Hz, 1H), 7.80 (d, J = 8.4 Hz, 2H), 7.69 (d, J = 11.9 Hz, 1H), 7.57 – 7.42 (m, 3H), 7.38 (s, 1H), 7.26 (d, J = 8.4 Hz, 2H), 7.08 – 6.95 (m, 1H), 6.45 (d, J = 5.2 Hz, 1H), 4.14 (t, J = 6.4 Hz, 2H), 3.94 (s, 5H), 3.83 (t, J = 8.6 Hz, 1H), 2.48 – 2.26 (m, 2H), 1.98 (t, J = 7.3 Hz, 2H), 1.81 (t, J = 7.3 Hz, 2H), 1.53 (q, J = 7.7 Hz, 2H), 1.46 (t, J = 7.7 Hz, 2H), 1.35 (q, J = 7.7 Hz, 2H). ^{13}C NMR (101 MHz, DMSO-d_6) δ 171.49 , 169.60 , 168.05 , 160.41 , 152.39 , 149.94 , 149.25 , 146.92 , 141.21 , 136.84 , 130.95 , 130.86 , 121.96 , 121.46 , 115.63 , 115.29 , 111.49 ,111.28 , 108.95 , 107.09 , 106.83 , 103.52 , 99.65 , 68.72 , 56.22 , 51.74 , 47.32 , 32.73 , 28.84 , 28.81 , 25.73 , 25.55 , 21.77 .

*4.1.12.3. N-(4-((7-((7-(hydroxyamino)-7-oxoheptyl)oxy)-6-methoxyquinolin-4-yl)oxy)phenyl)-2-oxo-1-phenylpyrrolidine-3-carboxamide (**15c**)*

Light yellow solid; Yield: 67.3%; M.p.: 132-134 ºC; MS (ESI) m/z(%): 613.15 $[M+H]^+$; ^{1}H NMR (400 MHz, DMSO-d_6) δ 10.47 (s, 1H), 10.35 (s, 1H), 8.67 (s, 1H), 8.46 (d, J = 5.2 Hz, 1H), 7.85 – 7.73 (m, 2H), 7.69 (d, J = 8.1 Hz, 2H), 7.51 (s, 1H), 7.40 (dd, J = 14.5, 6.5 Hz, 3H), 7.30 – 7.22 (m, 2H), 7.18 (t, J = 7.4 Hz, 1H), 6.45 (d, J = 5.2 Hz, 1H), 4.14 (t, J = 6.5 Hz, 2H), 4.02 – 3.85 (m, 5H), 3.80 (t, J = 8.6 Hz, 1H), 2.48 – 2.30 (m, 2H), 1.97 (t, J = 7.3 Hz, 2H), 1.81 (t, J = 7.4 Hz, 2H), 1.58 – 1.50 (m, 2H), 1.46 (t, J = 7.2 Hz, 2H), 1.35 (d, J = 7.2 Hz, 2H).

*4.1.12.4. 1-(3,4-difluorophenyl)-N-(4-((7-((7-(hydroxyamino)-7-oxoheptyl)oxy)-6-methoxyquinolin-4-yl)oxy)phenyl)-2-oxopyrrolidine-3-carboxamide (**15d**)*

Yellow solid; Yield: 39.0%; M.p.: 114-116 °C; MS (ESI) m/z (%): 649.19 $[M+H]^+$. ^{1}H NMR (400 MHz, DMSO-d_6) δ 10.50 (s, 1H), 10.36 (s, 1H), 8.69 (s, 1H), 8.46 (d, J = 5.2 Hz, 1H), 7.90 (ddd, J = 14.2, 7.5, 2.3 Hz, 1H), 7.80 (d, J = 8.6 Hz, 2H), 7.56 – 7.43 (m, 3H), 7.38 (s, 1H), 7.26 (d, J = 8.5 Hz, 2H), 6.45 (d, J = 5.3 Hz, 1H), 4.13 (q, J = 5.6, 4.7 Hz, 2H), 4.03 – 3.87 (m, 5H), 3.82 (t, J = 8.5 Hz, 1H), 2.43 (dd, J = 15.7, 6.8 Hz, 2H), 1.98 (t, J = 7.3 Hz, 2H), 1.81 (t, J = 7.3 Hz, 2H), 1.53 (q, J = 7.6 Hz, 2H), 1.50 – 1.42 (m, 2H), 1.35 (q, J = 7.7 Hz, 2H). ^{13}C NMR (101 MHz, DMSO-d_6) δ 171.38 , 169.58 , 168.04 , 160.41 , 152.42 , 149.94 , 149.29 , 146.92, 136.80 , 136.59 , 136.49 , 121.94 , 121.51 , 117.97 , 117.79 , 116.47 , 115.54 , 109.53 , 109.28 , 108.92 , 103.56 , 99.63 , 68.71 , 56.20 , 51.54 , 47.43 , 32.71 , 28.84 , 28.82 , 25.76 , 25.55 , 21.70 .

*4.1.12.5. N-(4-((7-((7-(hydroxyamino)-7-oxoheptyl)oxy)-6-methoxyquinolin-4-yl)oxy)phenyl)-2-oxo-1-(4-(trifluoromethoxy)phenyl)pyrrolidine-3-carboxamide (**15e**)*

White solid; Yield: 70.1%; M.p.: 171-172 ºC; MS (ESI) m/z(%): 697.07 $[M+H]^+$; ^{1}H NMR (400 MHz, DMSO-d_6) δ 10.51 (s, 1H), 10.36 (s, 1H), 8.69 (s, 1H), 8.46 (d, J = 5.1 Hz, 1H), 7.81 (dd, J = 8.7, 5.9 Hz, 4H), 7.52 (s, 1H), 7.48 – 7.33 (m, 3H), 7.26 (d, J = 8.2 Hz, 2H), 6.46 (d, J = 5.1 Hz, 1H), 4.14 (t, J = 6.4 Hz, 2H), 3.94 (m, 5H), 3.83

(m, 1H), 2.44 (d, J = 25.6 Hz, 2H), 1.98 (t, J = 7.3 Hz, 2H), 1.81 (t, J = 7.3 Hz, 2H), 1.55 (t, J = 7.4 Hz, 2H), 1.50 – 1.41 (m, 2H), 1.35 (d, J = 7.1 Hz, 2H).

*4.1.12.6. 1-(4-fluorophenyl)-N-(4-((7-((7-(hydroxyamino)-7-oxoheptyl)oxy)-6-methoxyquinolin-4-yl)oxy)phenyl)-2-oxopyrrolidine-3-carboxamide (**15f**)*

White solid; Yield: 62.2%; M.p.: 114-115 ºC; MS (ESI) m/z(%):631.21 $[M+H]^+$; ^{1}H NMR (400 MHz, DMSO-d_6) δ 10.48 (s, 1H), 10.35 (s, 1H), 8.67 (s, 1H), 8.46 (d, J = 5.2 Hz, 1H), 7.80 (d, J = 8.8 Hz, 2H), 7.74 – 7.65 (m, 2H), 7.51 (s, 1H), 7.38 (s, 1H), 7.25 (dt, J = 8.8, 4.5 Hz, 4H), 6.45 (d, J = 5.3 Hz, 1H), 4.14 (t, J = 6.5 Hz, 2H), 3.93 (d, J = 8.9 Hz, 5H), 3.79 (t, J = 8.6 Hz, 1H), 2.48 – 2.30 (m, 2H), 1.97 (t, J = 7.3 Hz, 2H), 1.81 (t, J = 7.3 Hz, 2H), 1.53 (q, J = 7.6 Hz, 2H), 1.46 (t, J = 7.6 Hz, 2H), 1.35 (q, J = 8.0 Hz, 2H).

*4.1.12.7. N-(4-((7-((7-(hydroxyamino)-7-oxoheptyl)oxy)-6-methoxyquinolin-4-yl)oxy)phenyl)-1-(2-methoxyphenyl)-2-oxopyrrolidine-3-carboxamide (**15g**)*

Yellow solid; Yield: 64.1%; M.p.: 105-106 °C; MS (ESI) m/z (%): 643.24 $[M+H]^+$; ^{1}H NMR (400 MHz, DMSO-d_6) δ 10.43 (s, 1H), 10.36 (s, 1H), 8.69 (s, 1H), 8.45 (d, J = 5.2 Hz, 1H), 7.80 (d, J = 8.5 Hz, 2H), 7.52 (s, 1H), 7.38 (s, 1H), 7.37 – 7.29 (m, 1H), 7.25 (dd, J = 8.3, 6.6 Hz, 3H), 7.13 (d, J = 8.2 Hz, 1H), 7.06 – 6.92 (m, 1H), 6.45 (d, J = 5.2 Hz, 1H), 4.14 (t, J = 6.5 Hz, 2H), 3.94 (s, 3H), 3.81 (s, 3H), 3.76 – 3.65 (m, 3H), 2.60 – 2.52 (m, 1H), 2.36 (d, J = 8.0 Hz, 1H), 1.98 (t, J = 7.3 Hz, 2H), 1.81 (t, J = 7.2 Hz, 2H), 1.59 – 1.51 (m, 2H), 1.47 (dq, J = 15.0, 8.4, 7.6 Hz, 2H), 1.35 (q, J = 7.7 Hz, 2H).

*4.1.12.8. N-(4-((7-((7-(hydroxyamino)-7-oxoheptyl)oxy)-6-methoxyquinolin-4-yl)oxy)phenyl)-1-(4-isopropylphenyl)-2-oxopyrrolidine-3-carboxamide (**15h**)*

White solid; Yield: 55.5%; M.p.: 148-150 ºC; MS (ESI) m/z(%): 655.27 $[M+H]^+$; ^{1}H NMR (400 MHz, DMSO-d_6) δ 10.47 (s, 1H), 10.35 (s, 1H), 8.68 (s, 1H), 8.46 (d, J = 4.0 Hz, 1H), 7.80 (d, J = 8.4 Hz, 2H), 7.66 – 7.56 (m, 2H), 7.52 (d, J = 2.6 Hz, 1H), 7.38 (s, 1H), 7.26 (p, J = 3.4 Hz, 4H), 6.46 (dd, J = 5.1, 2.6 Hz, 1H), 4.13 (d, J = 7.0 Hz, 2H), 3.93 (dd, J = 12.3, 5.2 Hz, 5H), 3.78 (m, 1H), 2.88 (m, 1H), 2.42 (m, 2H), 1.97 (d, J = 7.8 Hz, 2H), 1.88 – 1.70 (m, 2H), 1.50 (dt, J = 31.5, 7.6 Hz, 4H), 1.35 (m, 2H), 1.23 – 1.13 (m, 6H).

*4.1.12.9. 1-(3-chloro-4-fluorophenyl)-N-(4-((7-((7-(hydroxyamino)-7-oxoheptyl)oxy)-6-methoxyquinolin-4-yl)oxy)phenyl)-2-oxopyrrolidine-3-carboxamide (**15i**)*

Light yellow solid; Yield: 61.5%; M.p.: 148-149 ºC; MS (ESI) m/z(%):665.13 $[M+H]^+$; ^{1}H NMR (400 MHz, DMSO-d_6) δ 10.50 (s, 1H), 10.35 (s, 1H), 8.67 (s, 1H), 8.46 (d, J = 5.4 Hz, 1H), 7.99 (dd, J = 6.9, 2.7 Hz, 1H), 7.79 (d, J = 8.5 Hz, 2H), 7.67 (d, J = 9.0 Hz, 1H), 7.49 (dd, J = 16.4, 6.8 Hz, 2H), 7.38 (s, 1H), 7.26 (d, J = 8.5 Hz, 2H), 6.45 (d, J = 5.3 Hz, 1H), 4.14 (t, J = 6.7 Hz, 2H), 3.93 (d, J = 10.4 Hz, 5H), 3.81 (m, 1H), 2.43 (d, J = 17.0 Hz, 2H),

1.97 (t, J = 7.3 Hz, 2H), 1.81 (m, 2H), 1.61 – 1.51 (m, 2H), 1.46 (m, 2H), 1.38 – 1.31 (m, 2H).

*4.1.12.10. 1-(4-ethylphenyl)-N-(4-((7-((7-(hydroxyamino)-7-oxoheptyl)oxy)-6-methoxyquinolin-4-yl)oxy)phenyl)-2-oxopyrrolidine-3-carboxamide (**15j**)*

White solid; Yield: 52.4%; M.p.: 134-135 ºC; MS (ESI) m/z(%): 641.25 $[M+H]^-$; ^{1}H NMR (600 MHz, DMSO-d_6) δ 10.49 (s, 1H), 10.36 (s, 1H), 8.69 (s, 1H), 8.46 (d, J = 5.2 Hz, 1H), 7.80 (d, J = 8.5 Hz, 2H), 7.62 – 7.55 (m, 2H), 7.52 (s, 1H), 7.38 (s, 1H), 7.25 (dd, J = 12.1, 8.5 Hz, 4H), 6.45 (d, J = 5.2 Hz, 1H), 4.14 (t, J = 6.5 Hz, 2H), 3.99 – 3.84 (m, 5H), 3.78 (m, 1H), 2.59 (q, J = 7.6 Hz, 2H), 2.49 – 2.34 (m, 2H), 1.98 (t, J = 7.4 Hz, 2H), 1.81 (t, J = 7.4 Hz, 2H), 1.53 (q, J = 7.5 Hz, 2H), 1.46 (q, J = 7.7 Hz, 2H), 1.35 (q, J = 8.1 Hz, 2H), 1.17 (t, J = 7.6 Hz, 3H).

*4.1.12.11. N-(4-((7-((7-(hydroxyamino)-7-oxoheptyl)oxy)-6-methoxyquinolin-4-yl)oxy)phenyl)-2-oxo-1-(2-(trifluoromethoxy)phenyl)pyrrolidine-3-carboxamide (**15k**)*

Yellow solid; Yield: 47.3%; M.p.: 111-112 °C; MS (ESI) m/z (%): 697.20 $[M+H]^+$;^{1}H NMR (400 MHz, DMSO-d_6) δ 10.45 (s, 1H), 10.35 (s, 1H), 8.68 (s, 1H), 8.45 (d, *J* = 5.2 Hz, 1H), 7.85 – 7.72 (m, 2H), 7.60 – 7.43 (m, 5H), 7.38 (s, 1H), 7.31 – 7.19 (m, 2H), 6.45 (d, *J* = 5.2 Hz, 1H), 4.14 (t, *J* = 6.5 Hz, 2H), 3.94 (s, 3H), 3.87 – 3.77 (m, 2H), 3.73 (t, *J* = 8.5 Hz, 1H), 2.57 (ddd, *J* = 10.7, 7.6, 3.9 Hz, 1H), 2.48 – 2.34 (m, 1H), 1.97 (t, *J* = 7.3 Hz, 2H), 1.81 (p, *J* = 6.7 Hz, 2H), 1.54 (p, *J* = 7.5 Hz, 2H), 1.45 (q, *J* = 7.4 Hz, 2H), 1.35 (q, *J* = 7.7, 7.0 Hz, 2H).

*4.1.12.12. 1-(4-chlorophenyl)-N-(4-((7-((7-(hydroxyamino)-7-oxoheptyl)oxy)-6-methoxyquinolin-4-yl)oxy)phenyl)-2-oxopyrrolidine-3-carboxamide (**15l**)*

White solid; Yield: 73.5%; M.p.: 134-136 ºC; MS (ESI) m/z(%): 647.08 $[M+H]^+$; ^{1}H NMR (400 MHz, DMSO-d_6) δ 10.49 (s, 1H), 10.35 (s, 1H), 8.67 (d, *J* = 1.8 Hz, 1H), 8.46 (d, *J* = 5.2 Hz, 1H), 7.79 (d, *J* = 9.0 Hz, 2H), 7.73 (d, *J* = 9.0 Hz, 2H), 7.51 (s, 1H), 7.47 (d, *J* = 8.9 Hz, 2H), 7.38 (s, 1H), 7.26 (d, *J* = 9.0 Hz, 2H), 6.45 (d, *J* = 5.3 Hz, 1H), 4.14 (t, *J* = 6.5 Hz, 2H), 4.00 – 3.85 (m, 5H), 3.80 (t, *J* = 8.6 Hz, 1H), 2.44 (d, *J* = 8.2 Hz, 2H), 1.97 (t, *J* = 7.3 Hz, 2H), 1.81 (t, *J* = 7.4 Hz, 2H), 1.58 – 1.50 (m, 2H), 1.45 (m, 2H), 1.34 (m, 2H).

*4.1.12.13. 1-(4-bromophenyl)-N-(4-((7-((7-(hydroxyamino)-7-oxoheptyl)oxy)-6-methoxyquinolin-4-yl)oxy)phenyl)-2-oxopyrrolidine-3-carboxamide (**15m**)*

White solid; Yield: 66.5%; M.p.: 188-189 ºC; MS (ESI) m/z(%): 691.05 $[M+H]^+$; ^{1}H NMR (400 MHz, DMSO-d_6) δ 10.51 (s, 1H), 10.36 (s, 1H), 8.68 (s, 1H), 8.46 (d, *J* = 5.2 Hz, 1H), 7.80 (d, *J* = 8.4 Hz, 2H), 7.68 (d, *J* = 8.6 Hz, 2H), 7.59 (d, *J* = 8.7 Hz, 2H), 7.51 (s, 1H), 7.38 (s, 1H), 7.26 (d, *J* = 8.4 Hz, 2H), 6.45 (d, *J* = 5.2 Hz, 1H), 4.14 (t, *J* = 6.5 Hz, 2H), 3.94 (m, 5H), 3.81 (m, 1H), 2.47 – 2.24 (m, 2H), 1.97 (t, *J* = 7.3 Hz, 2H), 1.81 (t, *J* = 7.3 Hz, 2H), 1.50 (dt, *J* = 31.1, 7.5 Hz, 4H), 1.35 (m, 2H).

4.1.12.14. 1-(3-fluorophenyl)-N-(4-((7-((7-(hydroxyamino)-7-oxoheptyl)oxy)-6-methoxyquinolin-4-yl)oxy)phenyl)-

*2-oxopyrrolidine-3-carboxamide (**15n**)*

Yellow solid; Yield:72.5%; M.p.: 175-177 ºC; MS (ESI) m/z(%): 631.08 $[M+H]^+$; ^1H NMR (400 MHz, DMSO-d_6) δ 10.47 (s, 1H), 10.35 (s, 1H), 8.67 (s, 1H), 8.45 (s, 1H), 7.80 (d, J = 8.2 Hz, 2H), 7.49 (d, J = 10.9 Hz, 2H), 7.35 (d, J = 14.9 Hz, 3H), 7.26 (d, J = 8.3 Hz, 3H), 6.45 (d, J = 5.3 Hz, 1H), 4.13 (m, 2H), 3.93 (s, 3H), 3.85 (d, J = 8.6 Hz, 2H), 3.75 (m, 1H), 2.43 (m, 1H), 1.97 (m, 2H), 1.80 (m, 2H), 1.53 (m, 2H), 1.46 (m, 2H), 1.34 (m, 2H).

*4.1.12.15. 1-(2-bromophenyl)-N-(4-((7-((7-(hydroxyamino)-7-oxoheptyl)oxy)-6-methoxyquinolin-4-yl)oxy)phenyl)-2-oxopyrrolidine-3-carboxamide (**15o**)*

White solid; Yield: 84.2%; M.p.: 113-114 ºC; MS (ESI) m/z(%): 691.12 $[M+H]^+$; ^1H NMR (400 MHz, DMSO-d_6) δ 10.47 (s, 1H), 10.36 (s, 1H), 8.68 (s, 1H), 8.45 (d, J = 5.2 Hz, 1H), 7.87 – 7.68 (m, 3H), 7.56 – 7.46 (m, 2H), 7.43 (dd, J = 7.9, 1.8 Hz, 1H), 7.41 – 7.29 (m, 2H), 7.29 – 7.17 (m, 2H), 6.45 (d, J = 5.2 Hz, 1H), 4.13 (t, *J* = 6.5 Hz, 2H), 3.94 (s, 3H), 3.83 – 3.67 (m, 3H), 2.61 (dd, J = 12.7, 8.2 Hz, 1H), 2.47 – 2.36 (m, 1H), 1.97 (t, J = 7.3 Hz, 2H), 1.81 (t, J = 7.3 Hz, 2H), 1.59 – 1.50 (m, 2H), 1.50 – 1.41 (m, 2H), 1.39 – 1.27 (m, 2H).

*4.1.12.16. N-(4-((7-((7-(hydroxyamino)-7-oxoheptyl)oxy)-6-methoxyquinolin-4-yl)oxy)phenyl)-2-oxo-1-(m-tolyl)pyrrolidine-3-carboxamide (**15p**)*

White solid; Yield: 83.1%; M.p.: 147-149 ºC; MS (ESI) m/z(%): 627.17 $[M+H]^+$; ^1H NMR (400 MHz, DMSO-d_6) δ 10.46 (s, 1H), 10.34 (s, 1H), 8.70 – 8.60 (m, 1H), 8.46 (d, J = 5.3 Hz, 1H), 7.79 (d, J = 9.0 Hz, 2H), 7.56 – 7.42 (m, 3H), 7.38 (s, 1H), 7.27 (dd, J = 14.4, 8.4 Hz, 3H), 7.00 (d, J = 7.5 Hz, 1H), 6.45 (d, J = 5.2 Hz, 1H), 4.14 (t, *J* = 6.7 Hz, 2H), 4.01 – 3.85 (m, 5H), 3.78 (t, J = 8.6 Hz, 1H), 2.48 – 2.35 (m, 2H), 2.33 (s, 3H), 1.97 (t, J = 7.3 Hz, 2H), 1.81 (p, J = 6.4 Hz, 2H), 1.50 (dp, J = 30.3, 7.4 Hz, 4H), 1.40 – 1.28 (m, 2H).

*4.1.12.17. N-(3-fluoro-4-((7-((7-(hydroxyamino)-7-oxoheptyl)oxy)-6-methoxyquinolin-4-yl)oxy)phenyl)-2-oxo-1-phenylpyrrolidine-3-carboxamide (**15q**)*

Yellow green solid; Yield: 80.2%; M.p.: 160-162 ºC; MS (ESI) m/z(%): 631.21 $[M+H]^+$; ^1H NMR (400 MHz, DMSO-d_6) δ 10.73 (s, 1H), 10.37 (s, 1H), 8.69 (s, 1H), 8.50 (d, J = 5.4 Hz, 1H), 7.95 (dd, J = 12.9, 2.3 Hz, 1H), 7.69 (d, J = 8.1 Hz, 2H), 7.59 – 7.32 (m, 6H), 7.19 (t, J = 7.4 Hz, 1H), 6.52 (d, J = 5.3 Hz, 1H), 4.15 (t, J = 6.5 Hz, 2H), 4.04 – 3.86 (m, 5H), 3.82 (t, J = 8.6 Hz, 1H), 2.49 – 2.33 (m, 2H), 1.98 (t, J = 7.3 Hz, 2H), 1.81 (p, J = 6.9 Hz, 2H), 1.54 (p, J = 7.6 Hz, 2H), 1.46 (m, 2H), 1.35 (q, J = 7.9 Hz, 2H).

*4.1.12.18. 1-(2-fluorophenyl)-N-(4-((7-((7-(hydroxyamino)-7-oxoheptyl)oxy)-6-methoxyquinolin-4-yl)oxy)phenyl)-3-methyl-2-oxopyrrolidine-3-carboxamide (**15r**)*

White solid; Yield: 81.3%; M.p.: 104-106 ºC; MS (ESI) m/z(%): 645.10 $[M+H]^+$; ^1H NMR (600 MHz, DMSO-

d_6) δ 10.36 (s, 1H), 9.75 (s, 1H), 8.73 – 8.64 (m, 1H), 8.45 (d, J = 5.2 Hz, 1H), 7.80 (d, J = 8.5 Hz, 2H), 7.73 (dt, J = 11.9, 2.3 Hz, 1H), 7.51 (m, 2H), 7.47 (dd, J = 8.3, 6.8 Hz, 1H), 7.38 (s, 1H), 7.24 (d, J = 8.7 Hz, 2H), 7.03 (td, J = 8.3, 2.5 Hz, 1H), 6.44 (d, J = 5.2 Hz, 1H), 4.14 (t, J = 6.5 Hz, 2H), 3.94 (s, 3H), 3.90 (ddd, J = 14.5, 8.2, 5.9 Hz, 2H), 2.78 – 2.70 (m, 1H), 2.12 – 2.04 (m, 1H), 1.98 (t, J = 7.4 Hz, 2H), 1.81 (t, J = 7.5 Hz, 2H), 1.59 (s, 3H), 1.53 (q, J = 7.5 Hz, 2H), 1.50 – 1.41 (m, 2H), 1.35 (q, J = 8.3 Hz, 2H). ^{13}C NMR (151 MHz, DMSO-*d_6*) δ 174.54 , 170.36 , 169.61 , 160.39 , 152.37 , 150.09 , 149.91 , 149.24 , 146.88 , 141.28 ,136.56 , 130.92 , 130.86 ,122.49 , 121.74 , 115.73 , 115.52 , 111.51 , 108.90 , 107.20 , 107.03 , 99.60 , 68.66 , 56.19 , 55.37 , 54.37 , 45.75 , 32.70 , 30.02 , 28.81 , 25.76 , 25.55 , 21.53 .

*4.1.12.19. N-(4-((7-((7-(hydroxyamino)-7-oxoheptyl)oxy)-6-methoxyquinolin-4-yl)oxy)phenyl)-3-methyl-2-oxo-1-phenylpyrrolidine-3-carboxamide (**15s**)*

Yellow solid; Yield: 80.6%; M.p.:133-134 ºC; MS (ESI) m/z(%): 627.17 $[M+H]^+$; ^{1}H NMR (600 MHz, DMSO-*d_6*) δ 10.38 (s, 1H), 9.77 (s, 1H), 8.72 (s, 1H), 8.45 (d, J = 5.1 Hz, 1H), 7.81 (d, J = 8.3 Hz, 2H), 7.72 (d, J = 7.8 Hz, 2H), 7.51 (s, 1H), 7.42 (t, J = 7.6 Hz, 2H), 7.38 (s, 1H), 7.24 (d, J = 8.2 Hz, 2H), 7.19 (t, J = 7.2 Hz, 1H), 6.44 (d, J = 4.9 Hz, 1H), 4.13 (t, J = 6.4 Hz, 2H), 4.04 – 3.74 (m, 5H), 2.75 (dd, J = 13.9, 7.5 Hz, 1H), 2.08 (dd, J = 12.6, 6.1 Hz, 1H), 1.98 (t, J = 7.3 Hz, 2H), 1.81 (t, J = 7.3 Hz, 2H), 1.59 (s, 3H), 1.54 (t, J = 7.4 Hz, 2H), 1.46 (m, 2H), 1.35 (m, 2H). ^{13}C NMR (151 MHz, DMSO-*d_6*) δ 174.18 , 170.50 , 169.58 , 160.38 , 152.39 , 150.09 , 149.93 , 149.23 , 146.92 ,139.72 , 136.56 , 129.17 , 125.00 , 122.36 , 121.71 , 120.30 , 115.50 , 108.97 , 103.53 , 99.65 , 68.69 , 56.19 , 54.03 , 45.68 , 32.71 , 30.02 , 28.84 , 28.81 , 25.77 , 25.54 , 21.79 .

*4.1.12.20. 1-(4-chlorophenyl)-N-(4-((7-((7-(hydroxyamino)-7-oxoheptyl)oxy)-6-methoxyquinolin-4-yl)oxy)phenyl)-3-methyl-2-oxopyrrolidine-3-carboxamide (**15t**)*

White solid; Yield: 82.3%; M.p.: 139-141 ºC; MS (ESI) m/z(%): 661.03 $[M+H]^+$; ^{1}H NMR (600 MHz, DMSO-*d_6*) δ 10.36 (s, 1H), 9.75 (s, 1H), 8.68 (s, 1H), 8.46 (d, J = 5.3 Hz, 1H), 7.78 (dd, J = 16.9, 8.5 Hz, 4H), 7.51 (s, 1H), 7.48 (d, J = 8.6 Hz, 2H), 7.38 (s, 1H), 7.24 (d, J = 8.6 Hz, 2H), 6.44 (d, J = 5.2 Hz, 1H), 4.14 (t, J = 6.5 Hz, 2H), 3.94 (s, 3H), 3.92 – 3.80 (m, 2H), 2.79 – 2.67 (m, 1H), 2.08 (t, J = 5.1 Hz, 1H), 1.97 (t, J = 7.3 Hz, 2H), 1.80 (t, J = 7.4 Hz, 2H), 1.58 (s, 3H), 1.53 (m, 2H), 1.45 (q, J = 7.7 Hz, 2H), 1.34 (td, J = 8.3, 4.2 Hz, 2H). ^{13}C NMR (151 MHz, DMSO-*d_6*) δ 174.35 , 170.44 , 169.63 , 160.40 , 152.41 , 150.11 , 149.90 , 149.22 , 146.88 , 138.63 , 136.63 , 129.15 , 128.72 , 122.43 , 121.79 , 115.54 , 108.90 , 103.55 , 99.59 , 68.69 , 56.19 , 54.15 , 45.68 , 32.71 , 30.06 , 28.85 , 28.82 , 25.77 , 25.56 , 21.59 .

4.2. Pharmacology

4.2.1. In vitro antiproliferative assays

The antiproliferative activities of compounds **15a-15t** were evaluated against HCT-116, MCF-7 and A549 cell lines by the standard MTT assay in vitro, with SAHA, Cabozantinib and Foretinib as positive controls. The cancer cell lines were cultured in minimum essential medium (MEM) supplement with 10% fetal bovine serum (FBS). Approximate 4×10^3 cells, suspended in MEM medium, were plated into each well of a 96-well plate and incubated in 5% CO_2 at 37 °C for 24 h. The tested compounds at the indicated final concentrations were added to the culture medium and incubated for 72 h. Fresh MTT was added to each well at the terminal concentration of 5 μg/mL, and incubated with cells at 37 °C for 4 h. The formazan crystals in each well were dissolved in 100 μL DMSO, and the absorbency at 492 nm (for absorbance of MTT formazan) and 630 nm (for the reference wavelength) was measured with an ELISA reader. All of the compounds were tested three times in each of the cell lines. The results, expressed as IC_{50} (inhibitory concentration 50%), were the averages of three determinations and calculated relative to the vehicle (DMSO) control by the Bacus Laboratories Incorporated Slide Scanner (Bliss) software.

4.2.2 In vitro enzymatic assays

4.2.2.1 In vitro HDAC1 enzymatic assays

The following materials were purchased : HDAC1 (BPS, Cat. No. 50051), 384-well plate (Perkin Elmer, Cat. No. 6007279). The compounds were dissolved into 10 mM stock in 100% DMSO.

4.2.2.1.1 Experimental Methods

Prepare 1x assay buffer (modified Tris Buffer), then transfer compounds to assay plate by Echo in 100% DMSO. The final fraction of DMSO is 1%. Then we need to prepare enzyme solution in 1x assay buffer. Adding trypsin and Ac-peptide substrate in 1x assay buffer to make the substrate solution. Transfer 15 μL of enzyme solution to assay plate or for low control transfer 15 μL of 1x assay buffer. Reactions were incubated for 15 min at room temperature and added 10 μL of substrate solution to each well to start reaction. Read the plate on Synergy MX with excitation at 355 nm and emission at 460 nm after incubating for another 60 min at room temperature.

4.2.2.1.2 Curve fitting

Fit the data in Excel to obtain inhibition values using equation (1)

Equation (1): Inh %=(Max-Signal)/ (Max-Min)*100

Fit the data in XL-Fit to obtain IC_{50} values using equation (2)

Equation (2): Y=Bottom + (Top-Bottom)/(1+(IC_{50}/X)*HillSlope)

Y is %inhibition and X is compound concentration.

4.2.2.2 In vitro c-Met enzymatic assays

The target compounds were tested for their activity against c-Met Tyrosine kinases through the mobility shift

assay [38-39]. All kinase assays were performed in 96-well plates in a 50 μL reaction volume. The kinase buffer contains 50 mM HEPES, pH 7.5, 10 mM $MgCl_2$, 0.0015% Brij-35 and 2 mM DTT. The stop buffer contains 100 mM HEPES, pH 7.5, 0.015% Brij-35, 0.2% Coating Reagent 3 and 50 mM EDTA. Dilute the compounds to 500 μM by 100% DMSO, then transfer 10 μL of compound to a new 96-well plate as the intermediate plate, add 90 μL kinase buffer to each well. Transfer 5 μL of each well of the intermediate plate to 384-well plates. The following amounts of enzyme and substrate were used per well: kinase base buffer, FAM-labeled peptide, ATP and enzyme solution. Wells containing the substrate, enzyme, DMSO without compound were used as DMSO control. Wells containing just the substrate without enzyme were used as low control. Incubate at room temperature for 10 min. Add 10 μL peptide solution to each well. Incubate at 28 °C for specified period of time and stop reaction by 25 μL stop buffer. At last collect data on Caliper program and convert conversion values to inhibition values. Percent inhibition = (max − conversion)/(max − min)×100. 'max' stands for DMSO control; 'min' stands for low control.

4.2.3. Flow cytometry

The HCT-116 cells were seeded in 6-well plates at a seeding density of 105 cells per mL. Twelve hours later, various concentrations of compound **15f** were added. Cells were treated with compound **15f** for 48 h. Then cells were transferred to EP tubes and washed three times with PBS buffer. Then the procedures according to the operating instructions of the kit were followed. Ultimately, cell apoptosis was analyzed using Annexin-V and propidium iodide (PI) double staining by flow cytometry. Early apoptotic cells were defined as Annexin-V positive/PI negative, late apoptotic cells as Annexin-V/PI-double positive and necrotic cells as Annexin-V positive/PI positive.

4.2.4. Cell cycle distribution analysis

The effects of compounds on cell cycle progression were determined using a standard propidium iodide (PI) staining procedure followed by flow cytometry analysis. Briefly, HCT-116 cells were seeded in six-well plates (5×104/well) and then treated with different concentrations of **15f** for 48 h. The cells were collected and washed twice with ice cold PBS, then fixed in ice-cold 70% (v/v) ethanol overnight at 4 °C. The cells were washed again by PBS, and then the cell DNA was stained with 400 μL PI (Beyotime) for 10 min. Data acquisition and analysis were performed using a flow cytometer.

4.2.5. Molecular docking study

The crystal structure of c-Met (PDB entry code: 3LQ8) in complex with XL880 and HDACs (PDB entry code: 1C3S) in complex with SAHA were used for molecular modeling. The protein structures were prepared using the protein preparation wizard in Maestro with standard settings. Grids were generated using glide, version 4.5.208,

following the standard procedure recommended by Schrödinger software package version 2014. The conformational ensembles were docked flexibly using Glide with standard settings in both standard and extra precision mode. Only poses with low energy conformations and good hydrogen bond geometries were considered. The pictures elucidating the protein-ligand interactions were produced by Pymol (version 1.7.2.1).

Notes

The authors declare no competing financial interest.

Acknowledgements

This work was supported by grant (No. 81573295) from the National Natural Science Foundation of China and LiaoNing Revitalization Talents Program (XLYC1808037).

References

[1] Claiborne, C. F., Manfredi, M. G. Kinase Inhibitor Drugs. Eds.; John Wiley & Sons, Hoboken. **2009**.

[2] Burnett, G.; Kennedy, E. P. The Enzymatic Phosphorylation of Proteins. *J. Biol. Chem.* **1954**, 211, *969-980.*

[3] Pao, W.; Miller, V. A.; Politi, K. A.; Riely, G. J.; Somwar, R.; Zakowski, M. F.; Kris, M. G.; Varmus, H. Acquired Resistance of Lung Adenocarcinomas to Gefitinib or Erlotinib Is Associated with a Second Mutation in the EGFR Kinase Domain. *Plos Med*. **2015,** 2 (3), e73.

[4] Avizienyte, E.; Ward, R. A.; Garner, A. P. Comparison of the EGFR Resistance Mutation Profiles Generated by EGFR-Targeted Tyrosine Kinase Inhibitors and the Impact of Drug Combinations. *Biochem. J.* **2008**, 415, 197–206.

[5] Olgen S . Overview on Anticancer Drug Design and Development. *Curr Med Chem*, **2017**, 25, 1704-1719.

[6] Mokhtari, R. B.; Homayouni, T. S.; Baluch, N.; Morgatskaya, E.; Kumar, S.; Das, B.; Yeger, H. Combination Therapy in Combating Cancer. *Oncotarget*. **2017**, 8, 38022–38043.

[7] Anighoro, A.; Bajorath, J.; Rastelli, G. Polypharmacology: Challenges and Opportunities in Drug Discovery. *J. Med. Chem*. **2014**, 57, 7874–7887.

[8] Peters; Jens-Uwe. Polypharmacology – Foe or Friend? *J. Med. Chem*. **2013,** 56, 8955–8971.

[9] Boccaccio, C.; Comoglio, P. M. Invasive Growth: A MET -Driven Genetic Programme for Cancer and Stem Cells. *Nat. Rev. Cancer,* **2006**, 6, 637–645.

[10] Bottaro, D.; Rubin, J.; Faletto, D.; Chan, A.; Kmiecik, T.; Vande Woude, G.; Aaronson, S. Identification of the Hepatocyte Growth Factor Receptor as the C-Met Proto-Oncogene Product. *Science.* **1991**, 251, 802–804.

[11] Liao, Y.; Grobholz, R.; Abel, U.; Trojan, L.; Michel, M. S.; Angel, P.; Mayer, D. Increase of AKT/PKB Expression Correlates with Gleason Pattern in Human Prostate Cancer. *Int. J. Cancer.***2003***,* 107, 676–680.

[12] Kreisberg, J. I.; Malik, S. N.; Prihoda, T. J.; Bedolla, R. G.; Ghosh, P. M. Phosphorylation of Akt (Ser(473)) Is an Excellent Predictor of Poor Clinical Outcome in Prostate Cancer. *Cancer Res*. **2004**, 64, 5232–5236.

[13] Christensen, J. G.; Burrows, J.; Salgia, R. C-Met as a Target for Human Cancer and Characterization of Inhibitors for Therapeutic Intervention. *Cancer Letters*. **2005**, 225, 1-26.

[14] Cappuzzo, F.; Marchetti, A.; Skokan, M.; Rossi, E.; Gajapathy, S.; Felicioni, L.; Grammastro, M. D.; Sciarrotta, M. G.; Buttitta, F.; Incarbone, M.; Toschi, L.; Finocchiaro, G.; Destro, A.; Terracciano, L.;Roncalli, M.; Alloisio, M.; Santoro, A.; Varella-Garcia, M. Increased MET Gene Copy Number Negatively Affects Survival of Surgically Resected Non–Small-Cell Lung Cancer Patients. *J. Clin. Oncol*. **2009**, 27, 1667-1674.

[15] Li, S.; Huang, Q.; Liu, Y.; Zhang, X.; Gong, P. Design, Synthesis and Antitumour Activity of Bisquinoline Derivatives Connected by 4-Oxy-3-Fluoroaniline Moiety. *Eur. J. Med. Chem*. **2013**, 64, 62–73.

[16] Li, S.; Zhao, Y. F.; Wang, K. W.; Gao. Y. L.; Han, J. M.; Cui, B. B.; Gong, P. Discovery of novel 4-(2-fluorophenoxy)quinoline derivatives bearing 4-oxo-1,4-dihydrocinnoline-3-carboxamide moiety as c-Met kinase inhibitors. *Bioorg Med Chem*. **2013**, 21, 2843-2855.

[17] Organ, S. L.; Tsao, M.-S. An Overview of the C-MET Signaling Pathway. *Ther. Adv. Med. Oncol*. **2018**, 3, S7–S19.

[18] Xu WS, Parmigiani RB, Marks PA. Histone deacetylase inhibitors: molecular mechanisms of action. *Oncogene*. **2007**, 26, 5541–5552.

[19] Bose, P.; Dai, Y.; Grant, S. Histone Deacetylase Inhibitor (HDACI) Mechanisms of Action: Emerging Insights. *Pharmacol. Ther.* **2014**, *143*, 323–336.

[20] Grabarska, A.; Dmoszyńskagraniczka, M.; Nowosadzka, E.; Stepulak, A. [Histone Deacetylase Inhibitors - Molecular Mechanisms of Actions and Clinical Applications]. *Postepy Hig Med Dosw*. **2013**, 67, 722–735.

[21] Matsumoto, Y.; Motoki, T.; Kubota, S.; Takigawa, M.; Tsubouchi, H.; Gohda, E. Inhibition of Tumor–Stromal Interaction through HGF/Met Signaling by Valproic Acid. *Biochem Bioph Res Co*. **2008**, 366, 110–116.

[22] Carafa, V.; Miceli, M.; Altucci, L.; Nebbioso, A. Histone Deacetylase Inhibitors: A Patent Review (2009 – 2011). Expert Opin. Ther. Pat. *Expert Opin. Ther. Patents.* **2013**, 23,1-17

[23] J. P. Laubach, J. F. San-Miguel, V. Hungria, J. Hou,nP. Moreau, S. Lonial, J. H. Lee, H. Einsele, M. Alsina and P. G. Richardson. *Expert Rev. Hematol.* **2017**, 10, 229–237

[24] Hesham, H. M.; Lasheen, D. S.; Abouzid, K. A. M. Chimeric HDAC Inhibitors: Comprehensive Review on the HDAC-Based Strategies Developed to Combat Cancer. *Med. Res. Rev*. **2018**, 38, 2058-2109.

[25] Cai, X.; Zhai, H.-X.; Wang, J.; Forrester, J.; Qu, H.; Yin, L.; Lai, C.-J.; Bao, R.; Qian, C. Discovery of 7-(4-(3-Ethynylphenylamino)-7-Methoxyquinazolin-6-Yloxy)-*N*-Hydroxyheptanamide (CUDC-101) as a Potent Multi-Acting HDAC, EGFR, and HER2 Inhibitor for the Treatment of Cancer. *J. Med. Chem*. **2010**, *53*, 2000–2009.

[26] Sun, K.; Atoyan, R.; Borek, M. A.; Dellarocca, S.; Wang, J. Dual HDAC and PI3K Inhibitor CUDC-907 down Regulates MYC and Suppresses Growth of MYC-Dependent Cancers. *Mol. Cancer Ther.* **2016**, 16, 285-299.

[27] Mondello, P.; Derenzini, E.; Asgari, Z.; Philip, J.; Younes, A. Dual Inhibition of Histone Deacetylases and Phosphoinositide 3-Kinase Enhances Therapeutic Activity against B Cell Lymphoma. *Oncotarget.* **2017**, 8, 14017–14028.

[28] Study to Evaluate the Efficacy and Safety of CUDC-907 With and Without Rituximab in Subjects With RR MYC-Altered DLBCL (NCT02674750). https://clinicaltrials.gov/ct2/show/NCT02674750.**2016.**

[29] D. Lu, J. Yan, L. Wang, H. C. Liu, L.M. Zeng, M. M. Zhang, W. W. Duan, Y. C. Ji, J.C. Cao, M.Y. Geng, A. J. Shen, Y. H. Hu, Design, Synthesis, and Biological Evaluation of the First c-Met/HDAC Inhibitors Based on Pyridazinone Derivatives. *ACS. Med. Chem. Lett.* **2017**, 8, 830-834.

[30] Norman, M. H.; Liu, L.; Lee, M.; Xi, N.; Fellows, I.; D'Angelo, N. D.; Dominguez, C.; Rex, K.; Bellon, S. F.; Kim, T.-S. Structure-Based Design of Novel Class II c-Met Inhibitors: 1. Identification of Pyrazolone-Based Derivatives. *J. Med. Chem.* **2012**, 55, 1858–1867.

[31] Heinrich, T.; Seenisamy, J.; Blume, B.; Bomke, J.; Calderini, M.; Eckert, U.; Friese-Hamim, M.; Kohl, R.; Lehmann, M.; Leuthner, B. and. Discovery and Structure-Based Optimization of Next Generation Reversible Methionine Aminopeptidase-2 (MetAP-2) Inhibitors. *J. Med. Chem.* **2019**, 62, 5025-5039.

[32] Qian, F.; Engst, S.; Yamaguchi, K.; Yu, P.; Won, K.; Mock, L.; Lou, T.; Tan, J.; Li, C.; Tam, D. Inhibition of Tumor Cell Growth, Invasion, and Metastasis by EXEL-2880 (XL880, GSK1363089), a Novel Inhibitor of HGF and VEGF Receptor Tyrosine Kinases. *Cancer Res.* **2009**, 69, 8009–8016.

[33] Huang, Y.; Guoqiang, D.; Huanqiu, L.; Na, L.; Wannian, Z.; Chunquan, S. Discovery of Janus Kinase 2 (JAK2)

and Histone Deacetylase (HDAC) Dual Inhibitors as a Novel Strategy for Combinational Treatment of Leukemia and Invasive Fungal Infections. *J. Med. Chem.* **2018**, 61, 6056−6074.

[34] Zhu, X.; Gan, P. A Novel Synthesis of 1-Aminocyclopropane-1-Carboxylic Acid (ACC). *Synth. Commun.* **1998**, *28*, 3159–3162.

[35] Barreiro, E. J.; Kummerle, A. E.; Fraga, C. A. M. The Methylation Effect in Medicinal Chemistry. *Chem. Rev.* **2011**, 111, 5215–5246.

[36] Schonherr, H.; Cernak, T. Profound Methyl Effects in Drug Discovery and a Call for New CH Methylation Reactions. *Angew. Chem.* **2013**, 52, 12256–12267.

[37] Finnin, M. S.; Donigian, J. R.; Cohen, A.; Richon, V. M.; Rifkind, R. A.; Marks, P. A.; Breslow, R.; Pavletich, N. P. Structures of a Histone Deacetylase Homologue Bound to the TSA and SAHA Inhibitors. *Nature.* **1999**, 401, 188–193.

[38] Albrecht, B. K.; Harmange, J. C.; Bauer, D.; Berry, L.; Bode, C.; Boezio, A. A.; A. D. Chen.; Choquette, I. Dussault, C. Fridrich, R. Shimanovich, S. K. Springer, Y. Teffera, Y. Yang, Y. Zhang, S. F. Bellon, Discovery and optimization of triazolopyridazines as potent and selective inhibitors of the c-Met kinase, *J. Med. Chem.* **2008**, 51, 2879-2882.

[39] Liu, X.; Kou, J.; Xiao, Z.; Tian, F.; Hu, J.; Zheng, P.; Zhu,W.; Design, Synthesis and Biological Evaluation of 6,7-Disubstituted-4-phenoxyquinoline Derivatives Bearing Pyridazinone Moiety as c-Met Inhibitors. *Molecules*. **2018**, 23, 1543-1560.

- A series of novel c-Met/HDAC Dual Inhibitors were designed, synthesized.
- **15f** showed better cytotoxicity against tested cells and comparative enzymatic inhibitory than positive control.
- Cell apoptosis study revealed **15f** is very effective in the induction of apoptosis in a dose-dependent manner in HCT-116 cells.
- Cell cycle analysis showed that **15f** significantly caused G2/M-phase arrest in HCT-116 cells.
- Docking mode indicated **15f** could form critical bonding interactions with c-Met and HDAC1.

Graphical abstract

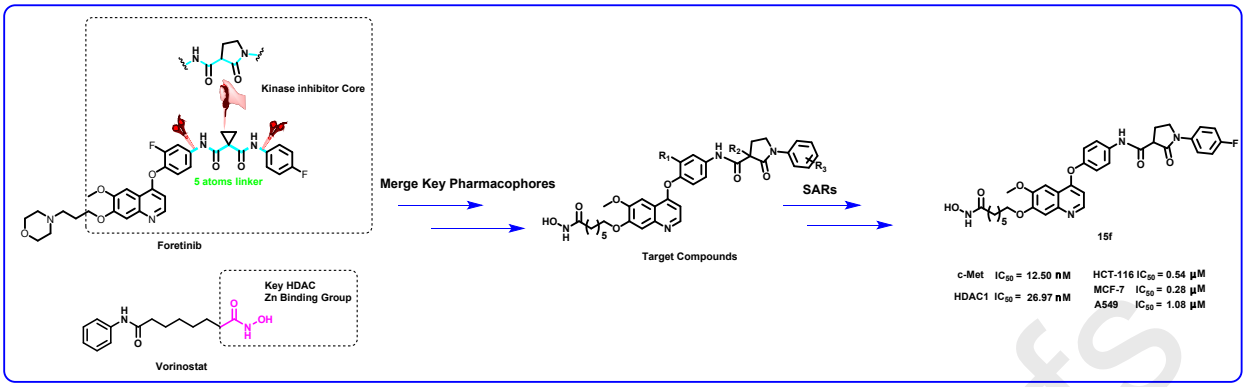

Dear editor,

We would like to submit the enclosed manuscript entitled "**Discovery of Novel Dual c-Met/HDAC Inhibitors as a Promising Strategy for Cancer Therapy**", which we wish to be considered for publication in "Bioorganic Chemistry". No conflict of interest exits in the submission of this manuscript, and manuscript is approved by all authors for publication. I would like to declare on behalf of my co-authors that the work described was our original research that has not been published previously and not under consideration for publication elsewhere, in whole or in part. All the authors listed have approved the manuscript that is enclosed.